**Department of Medicine, Albert Szent-Györgyi Medical School,
University of Szeged**

Myocardial mechanics in corrected tetralogy of Fallot

Gergely Rácz MD

PhD thesis

Tutor:

Prof. Attila Nemes MD, PhD, DSc

2024

Relevant publications

Full papers

I. Rácz G, Kormányos Á, Domsik P, Kalapos A, Gyenes N, Havasi K, Ambrus N, Hartyánszky I, Bogáts G, Nemes A. Left ventricular strains correlate with aortic elastic properties in adult patients with corrected tetralogy of Fallot (Results from the CSONGRAD Registry and MAGYAR-Path Study). Cardiovasc Diagn Ther. 2021 Apr; 11:611-622. **(Impact Factor: 2.552, Cardiology and Cardiovascular Medicine 2021: Q2)**

II. Nemes A, Rácz G, Kormányos Á, Domsik P, Kalapos A, Gyenes N, Ambrus N, Hartyánszky I, Bogáts G, Havasi K. Left ventricular rotational abnormalities in adult patients with corrected tetralogy of Fallot following different surgical procedures (Results from the CSONGRAD Registry and MAGYAR-Path Study). Cardiovasc Diagn Ther. 2021 Apr; 11:623-630. **(Impact Factor: 2.552, Cardiology and Cardiovascular Medicine 2021: Q2)**

III. Nemes A, Rácz G, Kormányos Á, Ambrus N, Havasi K. Tricuspid annular abnormalities following different surgical strategies in adults with corrected tetralogy of Fallot (Results from the CSONGRAD Registry and MAGYAR-Path Study). Cardiovasc Diagn Ther. 2021 Dec; 11:1276-1283. **(Impact Factor: 2.552, Cardiology and Cardiovascular Medicine 2021: Q2)**

IV. Rácz G, Zagyi A, Tóth A, Kormányos Á, Havasi K, Forster T, Nemes A. A műtétileg korrigált Fallot-tetralógiával élő felnőtt betegek multimodális képalkotó vizsgálata. Eredmények a CSONGRAD Regiszterből [Multimodality imaging of adult patients with surgically corrected tetralogy of Fallot. Results from the CSONGRAD Registry]. Orv Hetil. 2023 Feb; 164:186-194. **(Impact Factor: 0.707, Medicine (miscellaneous) 2023: Q4)**

Abstracts

I. Rácz G, Kormányos Á, Domsik P, Kalapos A, Gyenes N, Havasi K, Ambrus N, Hartyánszky I, Bogáts G, Kaemmerer H, Nemes A Left ventricular deformation and its relation to increased aortic stiffness in adult patients with corrected tetralogy of Fallot – Results from the CSONGRAD Registry and the three-dimensional speckle-tracking echocardiographic MAGYAR-Path Study. Cardiol Hung 2020; 50 Suppl D: p:143 (2020 Scientific Congress of the Hungarian Society of Cardiology)

II. Nemes A, Rácz G, Kormányos Á, Domsik P, Kalapos A, Gyenes N, Ambrus N, Hartyánszky I, Bogáts G, Havasi K, Left ventricular rotational abnormalities in adult patients with corrected tetralogy of Fallot following different surgical procedures – a three-dimensional speckle-tracking echocardiographic study. Eur Heart J 2020; 41 (Suppl 2): p:2184 (ESC Congress 2020)

Table of contents

Abbreviations

2D: two-dimensional
2DSTE: two-dimensional speckle-tracking echocardiography
3D: three-dimensional
3DS: three-dimensional strain
3DSTE: three-dimensional speckle-tracking echocardiography
AA: ascending Aorta
AD: aortic distensibility
AR: aortic regurgitation
ArS: area Strain
AS: aortic strain
ASI: aortic stiffness index
BMI: body mass index
BSA: body surface area
CHD: congenital heart disease
CI: confidence interval
cMR: cardiac magnetic resonance imaging
CS: circumferential strain
CSONGRÁD Registry: Registry for C(S)ONGenital caRdiAc Disease patients at the University of Szeged
DBP: diastolic blood pressure
DD: diastolic diameter
E and A: early and late diastolic transmitral flow velocities
ECG: electrocardiogram
EDV: end diastolic volume
EF: ejection fraction
ESC: European Society of Cardiology
ESV: end systolic volume
FAC: fractional area change
FOV: field of view
FTR: functional tricuspid regurgitation
IVS: interventricular septum
LA: left atrium
LS: longitudinal strain
LV: left ventricle
MA: mitral annulus
MAGYAR-Healthy Study: Motion Analysis of the heart and Great vessels bY three dimensionAl speckle-tRacking echocardiography in Healthy subjects Study
MAGYAR-Path Study: Motion Analysis of the heart and Great vessels bY three-dimensionAl speckle-tRacking echocardiography in Pathological cases Study
MR: mitral regurgitation
NYHA: New York Heart Association functional classification for heart failure
PR: pulmonic regurgitation
PS: pulmonic Stenosis
PW: posterior Wall
RA: right atrium
RBR: rigid body rotation
RS: radial strain
RT3DE: real-time three-dimensional echocardiography
RV: right ventricle
RVOT: right ventricular outflow tract
SBP: systolic blood pressure
SD: standard deviation
STE: speckle-tracking echocardiography
SV: stroke volume
TA: tricuspid annulus
TAA: tricuspid annular area
TAD: tricuspid annular diameter
TAFAC: tricuspid annular fractional area change
TAFS: tricuspid annular fractional shortening
TAP: tricuspid annular perimeter
TAPSE: tricuspid annular plane systolic excursion
TOF: tetralogy of Fallot
TOF: (surgically) corrected tetralogy of Fallot
etrTOF: patient with early total reconstructed TOF
pcTOF: patient with early palliated, late corrected TOF
TR: tricuspid regurgitation
VSD: ventricular septal defect

1. Introduction

Tetralogy of Fallot (TOF) is the most common (3–5%) cyanotic congenital heart disease (CHD), corresponding to one in 3,600 live births [1]. It is a conotruncal malformation characterised by the presence of a multilevel right ventricular (RV) outflow tract obstruction, leading to RV hypertrophy, and a ventricular septal defect (VSD) with overriding aorta [1]. The survival for untreated TOF was quite poor, but now it has a good prognosis due to timely follow-ups of residua, complications and well-timed interventions [1]. Due to advances in the surgical treatment of TOF in the last decades, almost all patients with correction (cTOF) can now expect to survive to adulthood [1]. Two surgical strategies are used in TOF patients in general: early palliation by creating artificial left-to-right shunts to provide adequate pulmonary blood flow followed by a late total reconstruction (pcTOF), or an early total reconstruction is performed (etrTOF) [2].

Aortopathy is a common phenomenon associated with CHD. The current literature considers coarctation of the aorta, bicuspid aortic valve, TOF, pulmonary atresia with VSD and truncus arteriosus to be the most important patient groups regarding the development of aortopathy, apart from genetic syndromes and secondary aortopathy is often seen after surgical repair including the Ross operation [3]. Aortic dilation in TOF is widely described and has been formerly associated with volume overload due to haemodynamic alterations in unrepaired TOF [1]. However, it is increasingly discussed that even late after surgical correction, abnormal dimensions and impaired elastic properties may be found in the ascending aorta in cTOF [4]. Further histopathologic studies have confirmed that there are intrinsic abnormalities in the aortic wall, which may be the cause of progressive aortic dilation and elastic abnormalities [5].

In recent two-dimensional (2D) speckle-tracking echocardiographic (STE) studies, during left ventricular (LV) strain analysis significant abnormalities in LV deformation could be detected in cTOF. It is of note, that deformation abnormalities can be present despite preserved LV ejection fraction (EF) and are rather a marker of subclinical dysfunction in otherwise largely asymptomatic patients. There are many different mechanisms attributed to these subclinical alterations described ranging from perioperative causes such as hypoxaemia, longstanding LV fibrosis, dysfunction of the pulmonary valve or the RV, as well as ventricular dyssynchrony as evidenced by broad QRS complex or right bundle branch block [6]. Furthermore, it is increasingly advised to incorporate deformation imaging into the clinical imaging of TOF. 2DSTE overcomes many limitations of previous methodologies and is now becoming widely available. While three-dimensional (3D) STE allows us to measure LV strain multidirectionally, thus not being limited to longitudinal strain and instead includes circumferential and radial deformation, as well as composite strains. Systolic deformation

impairment in patients with cTOF has been widely reported, however oftentimes only 2D-STE was utilised, and the understanding of the relation of the changes to surgical strategies is not widely established. It is nonetheless suggested in the literature - despite the heterogeneity of published studies - that the impairment of the LV deformation shows association with the EF, ventricular dyssynchrony, severity of the pulmonary valve disease and myocardial fibrosis, as well as - importantly - RV function. At the same time some data are available on the relationship of adverse clinical outcomes - primarily of sudden cardiac death and malignant arrhythmias, as well as heart failure - and LV deformation values. [7] There are some important studies which have shown reduced LV strains postoperatively after pulmonary valve replacement, while others have shown association of RV volume overload cause by pulmonary regurgitation (PR) and higher LV global strains. These results also highlight the importance of the interplay between the left and right hearts. [8] The suggested ventriculo-ventricular interdependence highlights the necessity of investigating similar relationships elsewhere in the heart of TOF patients as well. [7, 8]

As the more common strain-based measures of LV deformation such as longitudinal strain and other direction strains show significant abnormalities in cTOF, it is therefore perhaps not unexpected that the similarly STE derived measures LV rotation and twist are found to be altered. It is quite common for patients to have normal rotational patterns but at the same time having reduced overall twist. However abnormal rotational patterns have been described as well with either the abnormal rotation present apically, basally of both being affected. There are also some limited data available regarding the twisting velocities and peak torsion. At the same time the clinical relevance of these alterations is not yet fully established. [7] Moreover it has been suggested that LV rotational abnormalities might be inherent in TOF, can be detected in early childhood and are unrelated to the degree of PR and RV dilation. It is also intriguing to note that the expected maturation of LV deformation and the development of the normal LV twist can be disturbed in patients with cTOF. [9]

Despite the RV and the atria not being to focus of the present work, it is important to note that significant deformation abnormalities are present there as well. Most studies have shown reduced left atrial (LA) strains when compared to controls, in various phases of the cardiac cycle, with peak atrial reservoir strain being the most widespread parameter in clinical use. Furthermore, right atrial (RA) strains have been described as impaired in TOF when compared to healthy subjects. [8] A plethora of studies have investigated 2D-STE-based RV deformation imaging in TOF, and the widespread consensus has been established that RV free wall strain is reduced in cTOF patients when compared to controls. Some marked differences between the behaviour of the apical RV free wall and other areas have also been described suggesting its susceptibility adverse remodelling caused by abnormal

loading conditions and thus wall stress. RV deformation imaging has shown some clinical utility as a predictor of adverse outcomes, primarily of heart failure. [7,8]

As described above both aortopathy and LV dysfunction are shown to play an important role in the pathophysiology of TOF. Furthermore, it is also known that strong relationship exists between aortic and LV function called aorto-ventricular coupling. According to recent findings, aortopathy is thought to negatively influence LV function in CHD [10]. However, reports on the concurrent examination of both aortic and LV mechanics in TOF has been limited as of now.

Furthermore, both RV pressure and volume overload and RV dysfunction - which are commonly associated with TOF and are often present during its natural history - can lead to tricuspid annular (TA) dilation and functional tricuspid regurgitation (TR) may arise. Which in turn may exacerbate symptoms and is also a hallmark sign of disease progression [1, 11]. Thus, it is reasonable to expect some degree of TA dilation and dysfunction even before the appearance significant TR.
To add, cardiac magnetic resonance (cMR) has some additional value for the imaging of cTOF, as it has become the gold standard for precise quantification of the RV function and size as well as the degree of PR. Thus the application of multimodality imaging is of high importance in this CHD population. [1] Consequently we also examined the local application of the practice.

There are some not negligible knowledge gaps and challenges in the utilisation of these novel techniques nowadays. Despite ongoing efforts of standardisation, the assessment of LV and RV deformation and its reporting and interpretation has no gold standard in patients in cTOF. Significant heterogeneity exists in the type of used imaging modality and chosen deformation parameter. Also, important to add is that current CHD guidelines do not yet utilise STE-based deformation parameters. However, their incorporation would not be unexpected, similarly to the case of guideline indication for LV strain imaging in cardio-oncology. [7,8] The present thesis aims to provide some additions to the current understanding of myocardial mechanics in TOF and to facilitate the promotion of STE into widespread clinical practice in CHD.

2. Aims

1. To investigate LV strains and echocardiographic aortic elastic properties and their relationship in patients with cTOF late after early palliation/late correction (pcTOF) versus early total reconstruction (etrTOF).

2. To examine LV rotational mechanics, and its correlation with aortic elasticity in patients with cTOF late after pcTOF versus etrTOF.

3. To examine the tricuspid annulus, its dimensions and functional parameters in cTOF following pcTOF versus etrTOF.

To compare left and right heart parameters as assessed by echocardiography and cardiac magnetic resonance imaging of TOF patients following surgery. Clinical parameters were compared between cTOF patients undergoing etrTOF and pcTOF.

3. Methods

4. **Patient population (general considerations).** Complete 2D Doppler echocardiography and 3DSTE or cardiac magnetic resonance (cMR) imaging have been performed in all cases. In our department a registry was created to collect data of CHD patients treated and/or operated on at the Department of Pediatrics, Department of Heart Surgery, and 2nd Department of Medicine and Cardiology Center at the University of Szeged, Hungary since 1961. This is called the Registry of C(S)ONGenital caRdiAc Disease patients at the University of Szeged (CSONGRAD Registry), which involves data of more than 3,000 CHD patients [12]. Our results include the adult repaired TOF patients from the CSONGRAD Registry. The results are parts of the MAGYAR-Path Studies (Motion Analysis of the heart and Great vessels bY three-dimensionAl speckle-tRacking echocardiography in Pathological cases). These studies were organized at the Department of Medicine, University of Szeged to evaluate usefulness, diagnostic and prognostic value of 3DSTE-derived volumetric, strain, rotational etc. parameters in pathological cases and to establish their normal values and their physiological relationship with other normal parameters in healthy adults (’magyar’ means ’Hungarian’ in Hungarian language). Informed consent was obtained from each patient and the study protocol conformed to the ethical guidelines of the 1975 Declaration of Helsinki, as reflected in a prior approval by the institution’s human research committee (71/2011).

Two-dimensional echocardiography. Echocardiographic examinations were performed with a Toshiba Artida^{TM} cardiac ultrasound system (Toshiba Medical Systems, Tokyo, Japan) with a PST-30BT 1–5 MHz phased-array transducer, or a Philips Epiq 7G echocardiography imaging system (Philips, Eindhoven, The Netherlands) with a 1-5 MHz X5-1 sector transducer. The echocardiographic studies were stored digitally and underwent offline analysis. The experts who performed the analysis were unaware of the clinical data. Left and right heart dimensions and parameters, including LV, RV diameters, LV volumes, LV-EF, aortic and LA and RA sizes were all measured. These measurements were derived and averaged from 3 cardiac cycles. [13]

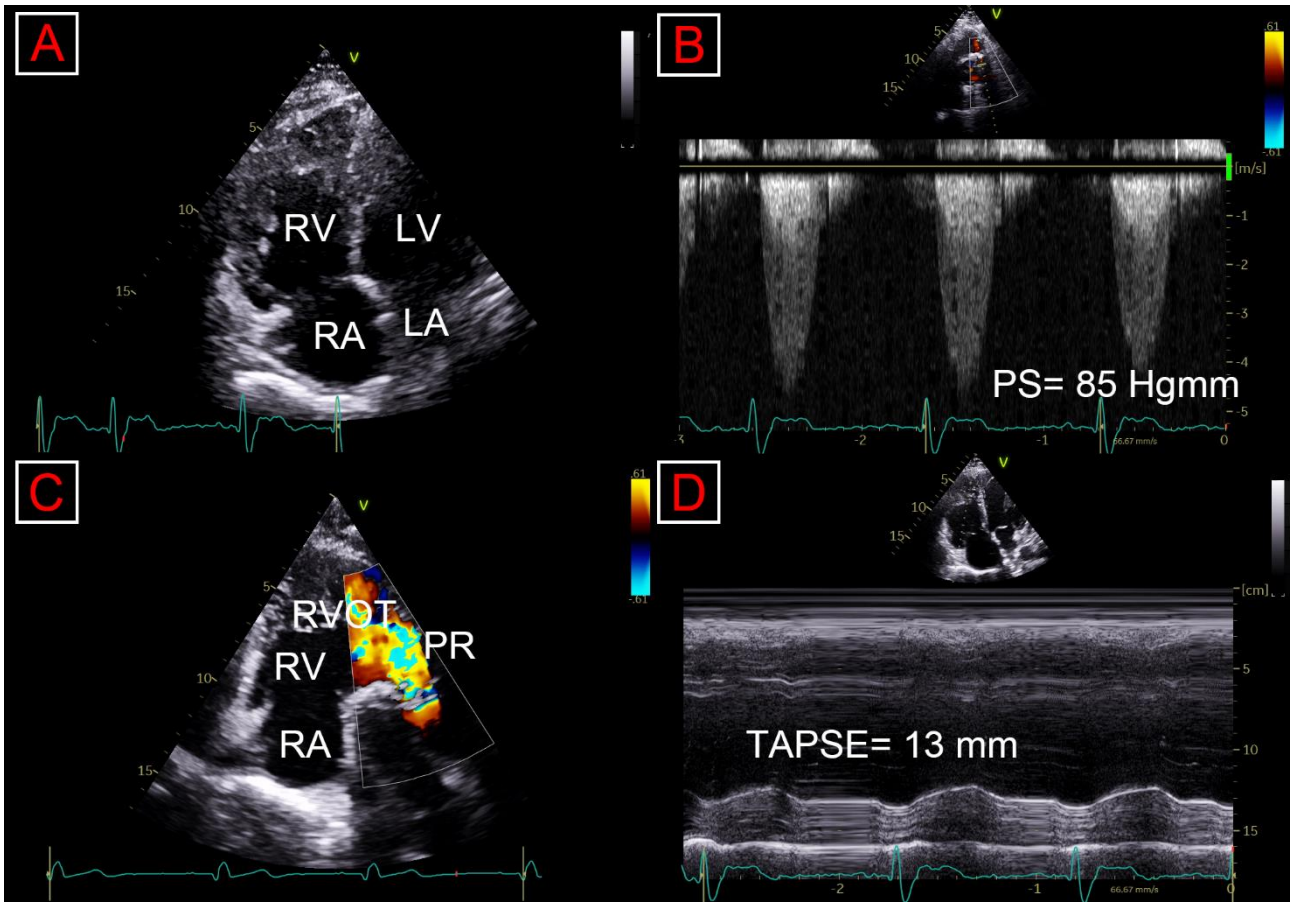

Figure 1. Echocardiographic images of a patient with tetralogy of Fallot. A) Echocardiographic image of tetralogy of Fallot from an apical right ventricle-focused four chamber view. Dilation and hypertrophy of the right ventricle is observed. B) Continuous wave Doppler curve of pulmonary homograft restenosis. C) Parasternal short-axis image with colour Doppler optimized for the pulmonary valve and right ventricular outflow tract, pulmonary regurgitation is large. D) Systolic displacement of the plane of the tricuspid annulus is reduced, demonstrating right ventricular dysfunction.

Abbreviations: RV: right ventricle, RA: right atrium, LV: left ventricle, LA: left atrium, RVOT: right ventricular outflow tract, PR: pulmonic regurgitation, PS: pulmonic stenosis, TAPSE: tricuspid annular plane systolic excursion

Measurement of blood pressure values. After 10 minutes of rest, patients were placed in a supine position, and with the cuff applied to the right arm, systolic and diastolic blood pressures (SBP and DBP, respectively) were measured. The first and fifth Korotkoff sounds were considered to indicate SBP and DBP. Patients did not consume caffeinated drinks or cigarettes before blood pressure measurements. [14]

Evaluation of aortic stiffness parameters. During standard transthoracic echocardiographic examination, ascending aortic diameters were recorded in parasternal long-axis view with M-mode 3 cm above the level of the aortic valve. Systolic and diastolic diameters (SD and DD) were measured at the maximum of the anterior motion of the aorta, and the peak of the QRS. Measurements were repeated 3 times and averaged. Aortic elastic properties have been calculated with the formulae bellow [14]:

- Aortic strain (AS) = (SD − DD)/DD;
- Aortic distensibility (AD) = 2 × (SD − DD)/[(SBP − DBP) × DD];
- Aortic stiffness index (ASI) = ln (SBP/DBP)/[(SD − DD)/DD] ("ln" is the natural logarithm)

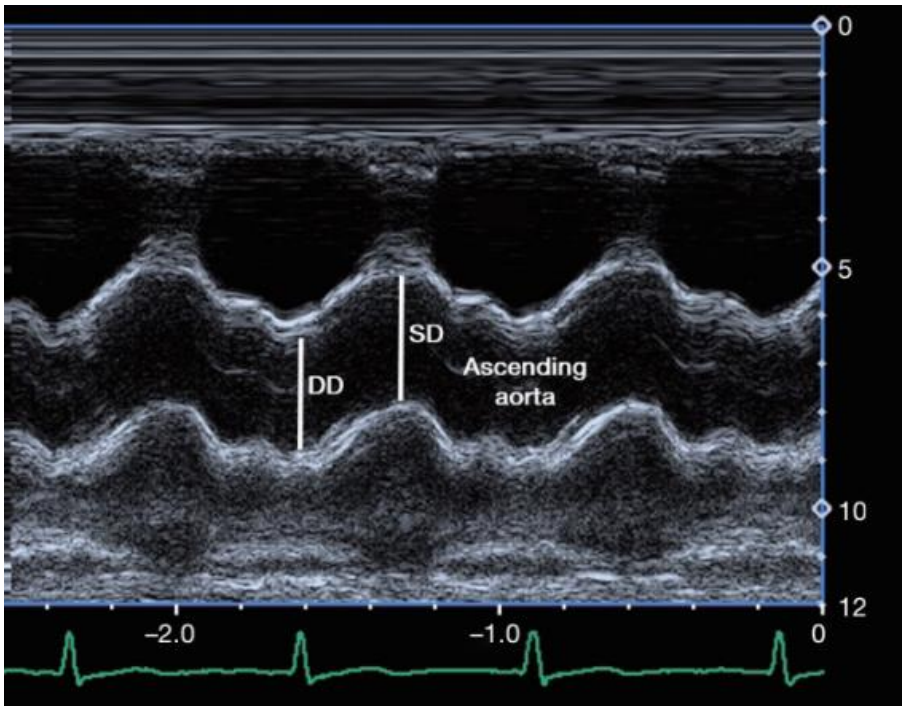

Figure 2 Measurements of systolic (SD) and diastolic (DD) diameters of the ascending aorta are presented in an M-mode echocardiographic image obtained 3 cm above the aortic valve.

3DSTE-derived data acquisition. 3D-STE studies were also performed with the same Toshiba Artida^{TM} echocardiographic system (Toshiba, Tokyo, Japan) using a 1–4 MHz matrix phased-array PST-25SX transducer placed in an apical window. Imaging depth, sector width, global and sector gain was all adjusted as necessary both to acquire the best possible image quality and to ensure the visibility of the structures under investigation. Frequency was not adjusted, the previously setup preset was utilized. The full pyramid-shaped dataset was created from 6 wedge-shaped subvolumes acquired with RR interval monitored by electrocardiogram (ECG), if remained the same. The acquired dataset underwent further offline analysis. [15, 16]

3DSTE-derived measurement of left ventricular strains. Quantification was performed using 3D Wall Motion Tracking software version 2.7 (Toshiba Medical Systems). At end-diastole, apical two- (AP2CH) and four-chamber (AP4CH) views and 3 short-axis views at different LV levels were automatically reconstructed from the acquired 3D echocardiographic cloud. The region of interest was then manually marked on the AP2CH and AP4CH views, with two points at the bases of the LV at the edges of the mitral annulus, and one at the endocardial surface of the LV apex (Figure 3). The reconstructed LV endocardial surface was then tracked during the cardiac cycle. 3D-STE-derived global (representing the whole LV) and segmental LV radial (RS, representing thickening/thining of the LV wall), circumferential (CS, representing widening/narrowing of the LV wall), longitudinal (LS, representing shortening/lengthening of the LV wall), area (AS) (combination of LS and CS) and 3D (3DS, combination of RA, LS and CS) strains were generated by the software.[15]

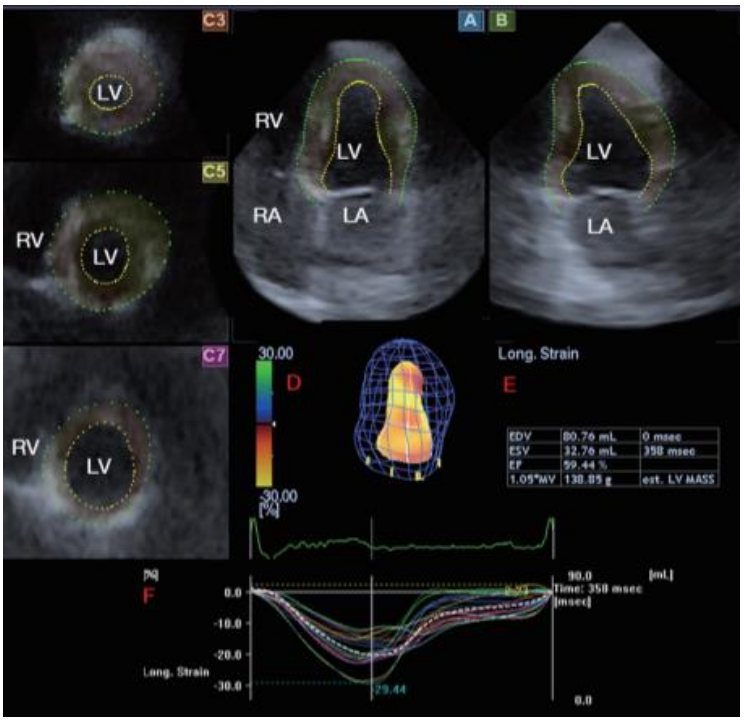

Figure 3. Three-dimensional (3D) speckle-tracking echocardiography-derived left ventricular (LV) strain analysis of a patient with corrected tetralogy of Fallot. The following views are presented: (A) apical four-chamber view, (B) apical two-chamber view, (C3) short-axis view at basal, (C5) mid- and (C7) apical LV level together with (D) 3D model of the LV and (E) LV volumetric data. Coloured curves represent time-LV segmental strains.

Abbreviations. LA: left atrium; LV: left ventricle; RA: right atrium; RV: right ventricle; EDV: end-diastolic volume; ESV: end-systolic volume; EF: ejection fraction.

3DSTE-derived analysis of the left ventricular rotational mechanics. Using the above mentioned cast of the LV, rotational parameters (apical and basal LV rotation and their absolute sum called LV twist) were calculated respecting the cardiac cycle. If apical and basal LV rotations were in the same direction, LV apico-basal gradient was measured.[16] (Figure 4)

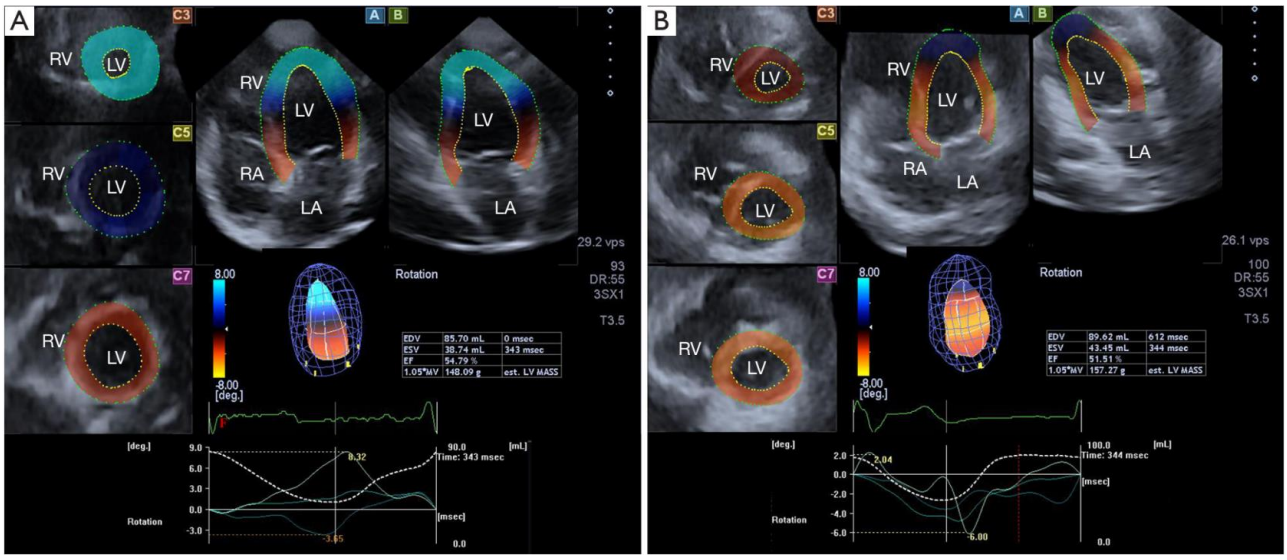

Figure 4 Three-dimensional (3D) speckle-tracking echocardiographic evaluation of left ventricular (LV) rotational parameters is presented in a patient with normally directed rotational mechanics (Panel A) and in a subject with apical and basal LV rotations in the same counterclockwise direction (LV 'rigid body rotation') (Panel B). Apical four-chamber (A) and two-chamber (B) LV views, cross-sectional views at different levels of the LV (C3, C5, C7), virtual 3D model of the LV and LV volumetric data are shown in both (Panel A) and (Panel B). Actual LV apical (white line), midventricular (light blue line) and basal (dark blue line) LV rotational curves and LV volume changes during a cardiac cycle (dashed white line) are also demonstrated.

Abbreviations. LA: left atrium; LV: left ventricle; RA: right atrium; RV: right ventricle; EDV: end-diastolic volume; ESV: end-systolic volume; EF: ejection fraction.

3DSTE-derived tricuspid annular measurements. For analysis of TA parameters, planes were optimized on long-axis views to create an 'en-face' view of the TA on C7 short-axis view (12) (Figure 5). End-diastolic (just before tricuspid valve closure) and end-systolic (just before tricuspid valve opening) measurements were performed for the evaluation of the following parameters:

TA morphological parameters

- TA diameter (TAD) = perpendicular line drawn from the peak of TA curvature to the middle of the straight TA border
- TA area (TAA), measured by planimetry
- TA perimeter (TAP), measured by planimetry

TA functional features

- TA fractional shortening (TAFS) = [(end-diastolic TAD − end-systolic TAD)/end-diastolic TAD] ×100
- TA fractional area change (TAFAC) = [(end-diastolic TAA − end-systolic TAA)/end-diastolic TAA] ×100.

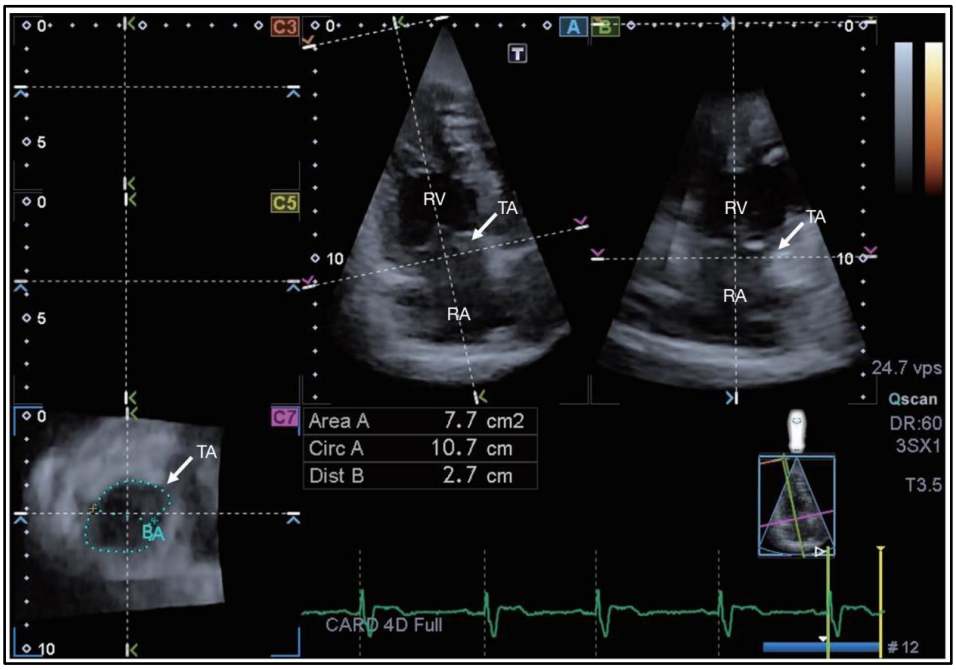

Figure 5 Images from a three-dimensional (3D) echocardiographic full-volume dataset in a patient with corrected tetralogy of Fallot: (A) apical four-chamber view; (B) apical two-chamber view and a cross sectional view at the level of the tricuspid annulus (C7) optimized on apical four- and two-chamber views. The arrow represents the TA plane on the long- (A, B) and short-axis (C7) images. **Abbreviations.** 3D: three-dimensional; RA: right atrium; RV: right ventricle; TA: tricuspid annulus.

3DSTE-derived measurement of RA volumes. For measurement of RA volumetric parameters, a 3D model of the RA was created by using the same software. Shortly, following image optimizations, edges of the TA and the endocardial side of the superior RA region were defined and then the endocardial RA surface was reconstructed by a sequential analysis. Using the 3D cast of the RA, the following volumetric RA parameters were calculated:

- Vmax: end-systolic RA volume [largest right atrium (RA) volume before tricuspid valve opening]
- VpreA: early diastolic RA volume (detected on ECG before atrial contraction at time of P wave)
- Vmin: late diastolic RA volume (smallest RA volume before tricuspid valve closure).

Cardiac magnetic resonance imaging. The current clinical gold standard for the determination of LV and RV EF, volumes and muscle mass is cMR. The studies were performed on Philips Achieva 1.5T Nova Dual HP (Philips, Best, The Netherlands) and Siemens MAGNETOM Aera 1.5T (Siemens, Erlangen, Germany) XQ MR machines. Using a retrospectively gated steady state free procession (SSFP) sequence in short and long-axis planes, motion images were projected in tilted views of the LV and RV outflow tracts, pulmonary divisions and branches, and the aortic and pulmonary/homograft valve. In addition, flow sensitive, phase-contrast motion-capture (cine) measurements were taken of the aorta and pulmonary/homograft valve and pulmonary branches in breath-hold. The amount of blood flowing through the slice can be determined at any cross-sectional area, and Qp/Qs and pulmonary differential flow can be non-invasively can be calculated. The study was complemented by a T2- prep (prepared) 3D b-SSFP/MRA sequence with fat suppression, with navigated diaphragm tracking in diastole, without contrast. The scan field of view (FOV: 24-40 cm) and slice thickness (4-8 mm) were adapted to the patient's body size. The spatial resolution of the moving images was better than 40 ms. The indexing of the data to the body surface allows a more reliable comparison of the parameters investiaged. In addition, a MassK value was calculated by applying a threshold in the cMR investigation, which, unlike the conventional evaluation, it considers the papillary muscles and trabeculae to the ventricular muscle mass. Accordingly, for cMR data, both values (papillary muscle/trabeculae included/not included) are shown. The evaluation software was Medis QMass and QFlow (Medis Medical Imaging, Leiden, The Netherlands).

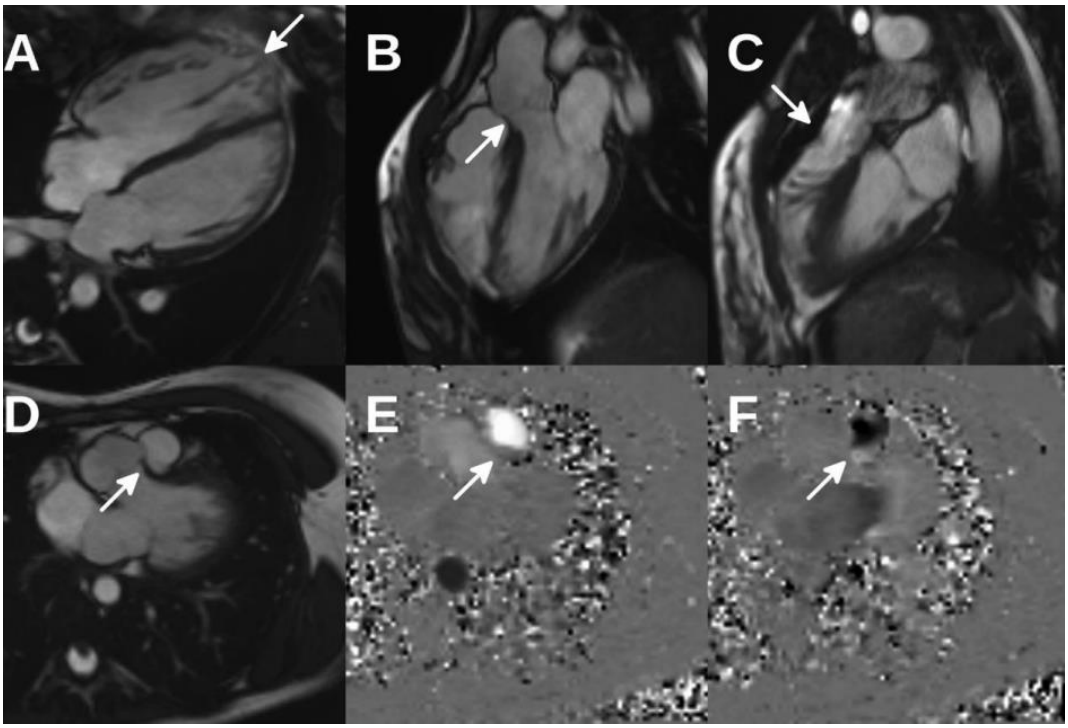

Figure 6. Cardiac magnetic resonance images of a patient with corrected tetralogy of Fallot. A) Four-chamber image in diastole, white arrow points to the volume overloaded right ventricle. B) Left ventricular outflow tract view in diastole, white arrow points to the repair patch of subaortic ventricular septal defect. C) Right ventricular outflow view in systole, white arrow: acceleration over pulmonary valve. D) View corresponding to pulmonary valve, white arrow: damaged valve, dorsally valve leaflet remnant. E) Measurement of phase contrast flow in systole on the pulmonary valve, white arrow: white colour code corresponding to the pulmonary valve indicates anterograde flow. F) Measurement of phase contrast flow at the pulmonary valve in diastole, white arrow: black colour code corresponding to the pulmonary valve indicates pulmonary insufficiency.

Statistical analysis. Continuous variables are reported as mean values ± standard deviation, while categorical data are summarized as frequencies and percentages. Comparisons were performed with Student t-test, $\chi 2$ test, and Fisher's exact test, when appropriate. Statistical significance was considered when the p value proved to be less than 0.05. Pearson's formula was used to determine numerical correlations. For statistical analysis Medcalc software (MedCalc, Mariakerke, Belgium) was used.

4. Results

4.1. Left ventricular strains correlate with aortic elastic properties in adult patients with corrected tetralogy of Fallot

Patient populations. Twenty-eight adult cTOF patients were involved in the present study who were followed-up with the help of CSONGRAD Registry, and who had repair at the age of 6.04±3.83 years. Of these patients, 15 underwent early palliative surgery [Blalock-Taussig (n=10), Waterston-Cooley (n=3) shunts, or Brock procedure (n=2)] and late total correction (pcTOF), while early total reconstruction was the treatment of choice in 13 cTOF patients (etrTOF). Their clinical parameters were compared to those of 39 age- and gender-matched healthy adults. There was no statistically significant difference in the presence of co-morbidities except for hypertension which was found in almost one third of cTOF patients. Body surface area was comparable in the patient and control groups. Detailed clinical and demographic data are presented in Table 1.

Two-dimensional echocardiographic data. Of the standard 2D echocardiographic parameters, LA diameter proved to be significantly larger in cTOF patients regardless of the treatment method. LV dimensions and function (except for LV end-systolic diameter) did not differ significantly between the groups examined. Significant (> grade 2) TR could be detected in 4 (15%) cTOF patients. None of the cTOF patients showed significant mitral regurgitation (MR). Aortic dimensions were somewhat dilated, AS and AD were reduced, while ASI proved to be increased in cTOF patients as compared to controls. When patients with different treatments were compared, etrTOF patients showed more beneficial aortic elastic properties compared to those of pcTOF patients (Table 1).

3DSTE-derived LV volumetric and strain data. For all cTOF patients 3DSTE-derived LV end-systolic volume (ESV) was higher and LV EF proved to be lower as compared to controls. Subgroup analysis showed that pcTOF patients had significantly larger LV-ESV and lower LV-EF than controls and etrTOF patients. cTOF patients showed significantly lower global and mean segmental LV-LS, LV-CS and LV-AS as compared to controls. In etrTOF patients global LV 3D strain (3DS) was higher than in controls. In pcTOF patients all global and mean segmental LV strains proved to be significantly lower as compared to those of etrTOF patients (Table 2). Segmental LV-LS, LV-CS, LV-RS, LV-AS and LV-3DS parameters are presented in Tables 3-7. Most segmental LV strains of pcTOF patients were significantly lower as compared to those of etrTOF patients and controls (Table 3-7)

Table 1 Comparison of baseline demographic, two-dimensional echocardiographic data and aortic elastic properties in different group of patients with tetralogy of Fallot and in controls

	Controls (n=39)	All cTOF (n=28)	etrTOF (n= 13)	pcTOF (n=15)
		Risk factors		
Age (years)	35.5 ±6.0	35 ±15.7	33.5±14.2	36.4±17.2
Female gender (%)	16 (41)	11 (39)	7 (54)	4 (27)
Hypertension (%)	0 (0)	8 (29)	4 (30)	4 (27)
Diabetes mellitus (%)	0 (0)	0 (0)	0 (0)	0 (0)
Hypercholesterolaemia (%)	0 (0)	1 (4)	1 (8)	0 (0)
Body surface area (m^2)	1.9 ±0.28	1.81 ±0.26	1.89±0.23	1.72±0.26
		Two-dimensional echocardiographic data		
LA diameter (mm)	35.3±4.21	41.9 ±7.0*	42.0 ±7.5*	41.8 ±6.8*
LV end-diastolic diameter (mm)	47.3 ±4.10	50.3 13.5	47.8 ±5.8	52.6 ±17.9
LV end-diastolic volume (ml)	104.1 ±24.24	110.0 ±33.5	108.8 ±32.7	111.0 ±35.0
LV end-systolic diameter (mm)	33.0 ±9.20	31.5 ±6.4*	31.2 ±5.3	31.7±7.6
LV end-systolic volume (ml)	36.6 ±9.03	42.3 ±26.9	39.5 ±20.3	44.8 ±32.5
Interventricular septum (mm)	9.2 ±1.48	9.7 ±1.5	9.5 ±1.1	9.9 ±1.8
LV posterior wall (mm)	9.4 ±1.79	9.5 ±1.4	9.4 ±1.4	9.6 ±1.5
LV ejection fraction (%)	64.2 ±3.54	63.9 ±11.2	65.5 ±6.1	62..4 ±14.5
		Aortic parameters		
Systolic aortic diameter (mm)	32.0 ±4.0	31.5 ±5.1	31.4 ±5.2	31.6 ±5.1
Diastolic aortic diameter (mm)	28.1 ±4.4	30.0 ±5.4	29.4 ±5.8	30.4 ±5.2
Systolic blood pressure (mmHg)	116.6 ±8.3	119.5 ±16.5	121.3 ±20.0	118.0 ±13.6
Diastolic blood pressure (mmHg)	80.3±4.8	78.9 ±10.7	82.9 ±12.6	75.7 ±7.9
Aortic strain	0.094± 0.046	0.057 ±0.048*	0.074 ±0.061	0.043 ±0.027*†
Aortic distensibility (cm^2/dynes 10^{-6})	2.74 ± 1.62	2.42±2.44*	3.25±3.24	1.76±1.33
Aortic stiffness index	7.21 ± 3.10	12.95 ± 11.25*	8.57 ± 5.38	16.46 ± 13.52*†

*** p<0.05 vs. controls, † p<0.05 vs. etrTOF**

Abbreviations: cTOF : corrected tetralogy of Fallot, etrTOF : early total reconstruction for patients with TOF, pcTOF : early pallication, late correction for patients with TOF, LA : left atrial, LV : left ventricular

Table 2 Comparison of three-dimensional speckle-tracking echocardiography-derived left ventricular volumetric parameters, global and mean segmental strains in different group of patients with tetralogy of Fallot and in controls

	Controls (n= 39)	All cTOF (n=28)	etrTOF (n= 13)	pcTOF (n=15)
		LV volumetric parameters		
LV-EDV (ml)	84.8 ±24.71	95.6 ±35.8	93.3 ±36.8	97.6 ±36.2
LV-ESV (ml)	35.6 ±15.5	53.6 ±33.7*	46.4 ±34.1	59.8 ±33.2*†
LV-EF (%)	57.9 ±5.49	46.9 ±14.1*	53.7 ±11.5	41.0 ±13.8*†
		global LV strains		
RS (%)	25.2 ±10.4	23.1 ±13.0	30.2 ±10.6	17.0 ±11.9*†
CS (%)	-27.6 ±4.9	-20.7 ±9.1*	-24.7 ±8.7	-17.3 ±8.2*†
LS (%)	-17.1 ±2.5	-14.8 ±4.0*	-15.6 ±3.2	-12.1 ±4.7*†
3DS (%)	27.7 ±10.1	25.5 ±12.6	32.7 ±10.2*	19.3 ±11.4*†
AS (%)	-40.5 ±4.9	-31.4 ±11.6*	-36.5 ±10.0	-27.0 ±11.4*†
		mean segmental LV strains		
RS (%)	27.4 ±10.4	26.9 ±12.7	33.8 ±10.1*	20.9 ±11.7*†
CS (%)	-28.5 ±5.0	-22.3 ±8.5*	-26.4 ±7.9	-18.7 ±7.6*†
LS (%)	-17.1 ±2.5	-14.8 ±4.0*	-16.8 ±2.4	-13.1 ±4.5*†
3DS (%)	29.7 ±10.0	28.7 ±12.6	35.9 ±10.0*	22.4 ±11.2*†
ArS (%)	-41.4 ±4.9	-33.2 ±10.6*	-38.4 ±8.6	-28.7 ±10.4*†

*** p<0.05 vs. controls, † p<0.05 vs. etrTOF**

Abbreviations: cTOF: corrected tetralogy of Fallot, etrTOF: early total reconstruction for patients with TOF, pcTOF: early pallication, late correction for patients with TOF, LV: left ventricular, 3DSTE: three-dimensional speckle-tracking echocardiography, RS: radial strain; CS: circumferential strain; LS: longitudinal strain; 3DS: three-dimensional strain, ArS: area strain

Table 3 Comparison of three-dimensional speckle-tracking echocardiography-derived left ventricular segmental radial strains in different group of patients with tetralogy of Fallot and in controls

	Controls (n= 39)	All cTOF (n=28)	etrTOF (n= 13)	pcTOF (n=15)
BA (%)	35.9 ±22.8	31.0 ±29.4	38.7 ±36.2	24.3 ±21.0
BAS (%)	39.6 ±20.3	31.7 ±22.3*	37.4 ±28.1	26.7 ±15.1*
BIS (%)	28.6 ±14.1	30.2 ±20.2	33.1 ±20.1	27.7 ±20.7
BI (%)	25.1 ±16.3	25.1 ±18.0	28.5 ±17.6	22.1 ±18.4
BIL (%)	29.7 ±21.4	21.8 ±13.9	24.6 ±15.6	19.3 ±12.3
BAL (%)	31.1 ±22.9	26.7 ±27.8	33.3 ±33.0	20.9 ±22.0
MAN (%)	31.1 ±18.1	32.5 ±28.1	41.7 ±28.2	24.5 ±26.4†
MAS (%)	34.6 ±15.2	30.5 ±20.2	39.8 ±21.2	22.5 ±15.9*†
MIS (%)	27.6 ±14.0	31.1 ±19.1	38.5 ±15.4*	24.7 ±20.1
MIN (%)	26.4 ±17.8	29.1 ±23.3	40.9 ±27.1*	19.0 ±13.3†
MIL (%)	29.6 ±21.9	29.4 ±24.3	42.3 ±26.6	18.2 ±15.6*†
MAL (%)	27.9 ±18.2	33.7 ±32.0	46.4 ±31.6	22.7 ±28.9†
AA (%)	16.6 ±11.4	16.9 ±12.1	18.7 ±12.5	15.3 ±11.9
ASE (%)	19.2 ±11.9	21.2 ±12.3	26.5 ±10.4*	16.7 ±12.2†
API (%)	19.6 ±15.5	19.5 ±19.6	27.6 ±22.1	12.5 ±14.4
AL (%)	16.5 ±11.4	19.9 ±22.5	23.3 ±22.6	17.0 ±22.8

*** p<0.05 compared to controls, † p<0.05 compared etrTOF**

Abbreviations: cTOF: corrected tetralogy of Fallot, etrTOF: early total reconstruction for patients with TOF, pcTOF: early pallication, late correction for patients with TOF, BA: basal anterior, BAS : basal anteroseptal, BIS: basal inferoseptal, BI: basal inferior, BIL: basal inferolateral, BAL: basal anterolateral, MAN: midventricular anterior, MAS: midventricular anteroseptal, MIS: midventricular inferoseptal, MIN: midventricular inferior, MIL: midventricular inferolateral, MAL: midventricular anterolateral, AA: apical anterior. ASE: apical septal, API: apical inferior, AL: apical lateral

Table 4. Comparison of three-dimensional speckle-tracking echocardiography-derived left ventricular segmental circumferential strains in different group of patients with tetralogy of Fallot and in controls

	Controls (n= 39)	All cTOF (n=28)	etrTOF (n= 13)	pcTOF (n=15)
BA (%)	-26.5 ±10.9	-15.9 ±8.4*	-17.7 ±10.7*	-14.3 ±5.5*
BAS (%)	-25.6 ±8.7	-17.7 ±9.6*	-22.8 ±10.0	-13.4 ±6.9*†
BIS (%)	-26.7 ±9.2	-18.5 ±10.0*	-20.7 ±8.3*	-16.7 ±11.1*
BI (%)	-21.4 ±8.9	-19.7 ±10.6	-22.3 ±11.0	-17.4 ±10.0
BIL (%)	-24.6 ±10.1	-25.4 ±10.4	-31.0 ±7.5*	-20.5 ±10.3†
BAL (%)	-28.3 ±10.8	-27.3 ±10.6	-31.6 ±7.4	-23.7 ±11.8†
MAN (%)	-28.1 ±9.9	-22.1 ±9.6*	-25.2 ±10.6	-19.4 ±7.9*
MAS (%)	-26.8 ±9.0	-19.5 ±11.3*	-25.1 ±11.0	-14.7 ±9.5*†
MIS (%)	-29.9 ±9.7	-20.6 ±11.2*	-25.8 ±10.4	-16.1 ±10.2*†
MIN (%)	-30.2 ±7.3	-24.7 ±12.2*	-30.0 ±11.5	-20.0 ±11.2*†
MIL (%)	-29.3 ±8.3	-24.7 ±11.4	-30.8 ±9.6	-19.5 ±10.3*†
MAL (%)	-32.2 ±9.9	-30.5 ±15.2	-35.6 ±14.6	-26.2 ±14.8*†
AA (%)	-26.4 ±13.0	-18.3 ±11.0*	-21.5 ±11.9	-15.5 ±9.6*
ASE (%)	-31.6 ±13.1	-23.3 ±15.8*	-29.1 ±17.8	-18.3 ±12.2*
API (%)	-34.1 ±10.9	-26.2 ±16.8*	-29.8 ±16.9	-23.0 ±16.6*
AL (%)	-33.5 ±12.2	-21.9 ±15.0*	-22.5 ±15.1*	-21.4 ±15.4*

*** p<0.05 compared to controls, † p<0.05 compared to etrTOF patients**

Abbreviations: cTOF: corrected tetralogy of Fallot, etrTOF: early total reconstruction for patients with TOF, pcTOF: early pallication, late correction for patients with TOF, BA: basal anterior, BAS : basal anteroseptal, BIS: basal inferoseptal, BI: basal inferior, BIL: basal inferolateral, BAL: basal anterolateral, MAN: midventricular anterior, MAS: midventricular anteroseptal, MIS: midventricular inferoseptal, MIN: midventricular inferior, MIL: midventricular inferolateral, MAL: midventricular anterolateral, AA: apical anterior. ASE: apical septal, API: apical inferior, AL: apical lateral

Table 5. Comparison of three-dimensional speckle-tracking echocardiography-derived left ventricular segmental longitudinal strains in different group of patients with tetralogy of Fallot and in controls

	Controls (n= 39)	All cTOF (n=28)	etrTOF (n= 13)	pcTOF (n=15)
BA (%)	-25.9 ±7.5	-15.6 ±5.2*	-18.4 ±4.7*	-13.1 ±4.3*†
BAS (%)	-18.1 ±5.9	-12.2 ±4.9*	-13.6 ±4.1*	-11.0 ±5.4*
BIS (%)	15.9 ±4.2	-15.8 ±6.1	-17.4 ±4.7	-14.4 ±6.9
BI (%)	-16.8 ±4.7	-18.7 ±6.5	-20.7 ±6.6	-16.9 ±6.0
BIL (%)	-18.2 ±6.7	-19.6 ±6.1	-22.4 ±6.2	17.1 ±5.0†
BAL (%)	-25.0 ±7.8	-19.4 ±7.4*	-22.6 ±6.2	-16.6 ±7.3*†
MAN (%)	-11.9 ±6.9	-15.3 ±7.1*	-17.4 ±7.2*	13.4 ±6.7
MAS (%)	-14.2 ±4.6	-11.9 ±5.2	-14.4 ±3.5	-9.7 ±5.5*†
MIS (%)	-14.7 ±4.0	-12.1 ±5.7	-14.4 ±5.8	-10.1 ±5.1*
MIN (%)	-14.9 ±4.5	-12.1 ±4.7	-14.3 ±4.1	-10.3 ±4.5*†
MIL (%)	-13.3 ±5.4	-12.2 ±5.7	-14.5 ±4.2	-10.2 ±6.2*†
MAL (%)	-14.3 ±6.1	-15.6 ±7.8	-18.5 ±7.5	-13.1 ±7.4†
AA (%)	-10.9 ±7.6	-8.4 ±6.5	-9.2 ±7.6	-7.7 ±5.7
ASE (%)	-24.4 ±9.4	-11.6 ±7.6*	-13.7 ±7.2*	-9.8 ±7.7*
API (%)	-23.6 ±8.2	-19.5 ±11.8	-20.6 ±11.7	-18.6 ±12.3
AL (%)	-11.6 ±7.0	-17.2 ±10,4*	-16.4 ±8.6	-17.9 ±12.1

*** p<0.05 compared to controls, † p<0.05 compared to etrTOF patients**

Abbreviations: : cTOF: corrected tetralogy of Fallot, etrTOF: early total reconstruction for patients with TOF, pcTOF: early pallication, late correction for patients with TOF, BA: basal anterior, BAS : basal anteroseptal, BIS: basal inferoseptal, BI: basal inferior, BIL: basal inferolateral, BAL: basal anterolateral, MAN: midventricular anterior, MAS: midventricular anteroseptal, MIS: midventricular inferoseptal, MIN: midventricular inferior, MIL: midventricular inferolateral, MAL: midventricular anterolateral, AA: apical anterior. ASE: apical septal, API: apical inferior, AL: apical lateral

Table 6. Comparison of three-dimensional speckle-tracking echocardiography-derived left ventricular segmental area strains in different group of patients with tetralogy of Fallot and in controls

	Controls (n= 39)	All cTOF (n=28)	etrTOF (n= 13)	pcTOF (n=15)
BA (%)	-44.5 ±10.8	-28.2 ±9.8*	-31.6 ±10.0*	-25.3 ±8.8*
BAS (%)	-39.2 ±8.6	-26.9 ±10.5*	-32.7 ±9.8*	-21.9 ±8.5*†
BIS (%)	-38.0 ±9.7	-30.8 ±11.4*	-34.3 ±9.2	-27.7 ±12.5*
BI (%)	-34.7 ±8.5	-35.0 ±10.6	-39.0 ±9.0	-31.5 ±10.9
BIL (%)	-38.0 ±10.8	-40.2 ±11.7	-47.3 ±5.8*	-34.0 ±12.3†
BAL (%)	-46.0 ±9.5	-41.6 ±12.8	-47.7 ±8.8	-36.2 ±13.6*†
MAN (%)	-37.3 ±12.3	-32.6 ±13.4	-36.6 ±14.2	-29.1 ±12.0
MAS (%)	-39.6 ±9.0	-28.5 ±13.4*	-35.8 ±11.1	-22.1 ±12.2*†
MIS (%)	-40.3 ±9.7	-29.2 ±13.9*	-36.1 ±12.2	-23.3 ±12.8*†
MIN (%)	-40.5 ±7.4	-33.0 ±14.1*	-39.4 ±13.2	-27.4 ±12.6*†
MIL (%)	-39.8 ±7.3	-33.2 ±13.7*	-40.8 ±9.5	-26.5 ±13.5*†
MAL (%)	-43.0 ±10.7	-40.0 ±17.6	-45.7 ±17.7	-34.9 ±16.5*
AA (%)	-36.4 ±15.0	-25.0 ±13.9*	-28.3 ±14.8	-22.2 ±13.0*
ASE (%)	-49.4 ±14.4	-32.0 ±19.0*	-38.8 ±20.2	-26.1 ±16.4*
API (%)	-49.9 ±11.3	-39.3 ±22.0	-43.3 ±20.9	-35.9 ±23.1*
AL (%)	-43.1 ±13.3	-33.2 ±10.6	-36.4 ±18.6	-35.0 ±22.4

*** p<0.05 compared to controls, † p<0.05 compared to etrTOF patients**

Abbreviations: : cTOF: corrected tetralogy of Fallot, etrTOF: early total reconstruction for patients with TOF, pcTOF: early pallication, late correction for patients with TOF, BA: basal anterior, BAS : basal anteroseptal, BIS: basal inferoseptal, BI: basal inferior, BIL: basal inferolateral, BAL: basal anterolateral, MAN: midventricular anterior, MAS: midventricular anteroseptal, MIS: midventricular inferoseptal, MIN: midventricular inferior, MIL: midventricular inferolateral, MAL: midventricular anterolateral, AA: apical anterior. ASE: apical septal, API: apical inferior, AL: apical lateral

Table 7. Comparison of three-dimensional speckle-tracking echocardiography-derived left ventricular segmental three-dimensional strains in different group of patients with tetralogy of Fallot and in controls

	Controls (n= 39)	All cTOF (n=28)	etrTOF (n= 13)	pcTOF (n=15)
BA (%)	38.3 ±23.7	32.2 ±28.9	39.9 ±35.7	25.5 ±20.4
BAS (%)	40.4 ±20.3	32.9 ±22.0	38.6 ±27.4	27.9 ±15.4*
BIS (%)	30.1 ±14.3	31.6 ±18.8	34.9 ±18.9	28.7 ±18.8
BI (%)	28.8 ±14.8	28.1 ±17.6	32.3 ±15.2	24.5 ±19.3
BIL (%)	36.9 ±20.3	26.4 ±14.0*	29.4 ±15.5	23.9 ±12.5*
BAL (%)	34.0 ±21.2	30.2 ±27.5	37.7 ±33.5	23.7 ±20.1
MAN (%)	31.7 ±18.0	33.5 ±26.5	43.2 ±27.1	25.2 ±23.8
MAS (%)	35.4 ±14.9	31.8 ±19.5	41.1 ±19.6	23.8 ±16.1*†
MIS (%)	28.9 ±13.9	32.1 ±17.9	39.7 ±14.3*	25.4 ±18.5†
MIN (%)	27.7 ±17.2	30.2 ±22.9	41.8 ±26.4*	20.1 ±13.5†
MIL (%)	32.5 ±21.0	30.9 ±22.5	43.6 ±23.9	19.9 ±14.5*†
MAL (%)	29.4 ±18.2	35.4 ±31.3	48.7 ±31.8	23.9 ±26.8†
AA (%)	17.5 ±11.6	18.4 ±12.3	20.7 ±12.2	16.4 ±12.4
ASE (%)	21.0 ±12.3	23.2 ±11.9	29.0 ±10.0*	18.2 ±11.5†
API (%)	21.2 ±15.5	20.7 ±19.2	29.4 ±21.7	13.1 ±13.2†
AL (%)	18.7 ±12.1	21.0 ±22.0	24.9 ±23.2	17.7 ±21.1

*** p<0.05 compared to controls, † p<0.05 compared to etrTOF patients**

Abbreviations: : cTOF: corrected tetralogy of Fallot, etrTOF: early total reconstruction for patients with TOF, pcTOF: early pallication, late correction for patients with TOF, BA: basal anterior, BAS : basal anteroseptal, BIS: basal inferoseptal, BI: basal inferior, BIL: basal inferolateral, BAL: basal anterolateral, MAN: midventricular anterior, MAS: midventricular anteroseptal, MIS: midventricular inferoseptal, MIN: midventricular inferior, MIL: midventricular inferolateral, MAL: midventricular anterolateral, AA: apical anterior. ASE: apical septal, API: apical inferior, AL: apical lateral

Correlations. Correlation coefficients between 3DSTE-derived strains and aortic elastic properties are demonstrated in Table 8. In all cTOF patients, several moderate correlations could be detected between LV strain parameters and aortic elastic properties. The subgroup analysis showed moderate correlations between LV-CS, LV-LS and LV-AS and AD in etrTOF patients. In pcTOF patients, only LV-RS correlated with aortic strain and LV-CS with ASI.

Table 8 Correlations between aortic elastic properties and left ventricular global strains in different group of patients with tetralogy of Fallot and in controls

	Aortic strain	Aortic distensibility	Aortic stiffness index
		In all cTOF patients	
global LV-RS	0.447*	0.327	-0.417*
global LV-CS	-0.416*	-0.477*	0.449*
global LV-LS	-0.339	-0.339	0.354
global LV-3DS	0.456*	0.344	-0.433*
global LV-ArS	-0.395*	-0.427*	0.422*
		In etrTOF patients	
global LV-RS	0.464	0.322	0.036
global LV-CS	-0.422	-0.576*	0.554
global LV-LS	-0.470	-0.591*	0.517
global LV-3DS	0.466	0.338	0.036
global LV-ArS	-0.460	-0.601*	0.567
		In pcTOF patients	
global LV-RS	0.535*	0.371	-0.480
global LV-CS	-0.320	-0.287	0.596*
global LV-LS	-0.149	-0.009	0.328
global LV-3DS	0.496	0.342	-0.462
global LV-ArS	-0.229	-0.141	0.492

*** Significance level of the correlation: p<0.05**

Abbreviations: cTOF: corrected tetralogy of Fallot, etrTOF : early total reconstruction for patients with TOF, pcTOF : early pallication, late correction for patients with TOF, LV:LeftVentricular

4.2. Left ventricular rotational abnormalities in adult patients with corrected tetralogy of Fallot following different surgical procedures

Patient population. The study prospectively involved 26 adult cTOF patients without pacemaker, who were willing to participate in this study. All data of these patients originate from the CSONGRAD Registry. Their results were compared to those of 37 age- and gender-matched healthy adults. From the 26 adult cTOF patients 14 had palliative surgery first [modified Blalock-Taussig (n=10), Waterston-Cooley (n=2) shunts, or Brock procedure (n=2)] (mean age at the palliation: 2.3±2.3 years, median age: 1.5 years, interquartile range: 3.5 years) and a late total correction (mean age at the total correction: 11.6±13.1 years, median age: 7.0 years, interquartile range: 6.0 years) (pcTOF), while the early total correction was the treatment of choice in 12 patients (mean age at the repair: 4.2±3.1 years, median age: 5.0 years, interquartile range: 5.3 years) (etrTOF). One quarter of cTOF patients showed hypertension regardless of previous procedure. Data are presented in Table 9.

Two-dimensional Doppler echocardiographic data. Dilated LA and smaller LV end-systolic diameter could be demonstrated in cTOF patients. The TAPSE and RV-FAC values of cTOF patients were 17.9±4.7 mm and 35.1 % ± 3.3 %, respectively. Significant (> grade 2) tricuspid regurgitations (TR) could be detected in 4 (15.4%) cTOF patients. None of the cTOF patients showed significant mitral and pulmonary (PR) regurgitation. Mean RV pressure was 14.8±2.3 mmHg without residual pulmonary stenosis or branch pulmonary artery narrowing. Data are presented in Table 9.

Aortic stiffness parameters. Most of our patients had normal aortic dimensions for adults with cTOF, and only 3 had larger than 35 mm, but less than 40 mm systolic aortic diameter. Reduced AS and AD and increased ASI could be detected in cTOF patients as compared to controls. When etrTOF and pcTOF patients were compared, etrTOF patients showed more beneficial aortic stiffness parameters than pcTOF patients. Data are presented in Table 9.

Table 9 Comparison of demographic, two-dimensional echocardiographic data and aortic elastic properties in patients with tetralogy of Fallot and in controls

	Controls (n=37)	All cTOF (n=26)	etrTOF (n= 12)	pcTOF (n=14)
Demographic data				
Age (years)	36.2 ±7.0	32.9 ±14.0	31.4±12.7	34.1±15.4
Female gender (%)	18 (48)	10 (38)	7 (58)	3 (21)
Hypertension (%)	0 (0)	6 (23)	3 (25)	3 (21)
Diabetes mellitus (%)	0 (0)	0 (0)	0 (0)	0 (0)
Hypercholesterolaemia (%)	0 (0)	1 (4)	1 (8)	0 (0)
Body surface area (m^2)	1.83 ±0.25	1.82 ±0.26	1.91±0.23	1.71±0.25
Two-dimensional echocardiographic data				
LA diameter (mm)	37.9±3.51	41.3 ±6.8*	41.8 ±7.8	40.8 ±6.0
LV end-diastolic diameter (mm)	48.1 ±3.02	50.2 ±13.8	48.2 ±5.9	52.1 ±18.5
LV end-diastolic volume (ml)	106.9 ±19.76	107.9 ±31.1	110.7 ±33.4	105.4 ±29.8
LV end-systolic diameter (mm)	33.8 ±10.36	31.0 ±5.7*	31.5 ±5.4	30.5±6.2*
LV end-systolic volume (ml)	37.1 ±7.4	39.0 ±20.0	40.4 ±20.9	37.8 ±19.9
Interventricular septum (mm)	9.0 ±1.1	9.7 ±1.5	9.5 ±1.1	9.9 ±1.9
LV posterior wall (mm)	9.2 ±1.1	9.5 ±1.5	9.4 ±1.4	9.5 ±1.6
LV ejection fraction (%)	65.3 ±2.42	65.3 ±8.6	65.3 ±6.3	65.2 ±10.5
Aortic parameters				
Systolic aortic diameter (mm)	29.5 ± 3.9	31.2±5.1	31.3±5.4	31.1±5.0
Diastolic aortic diameter (mm)	26.1 ± 5.4	29.6±5.4	29.3±6.0	29.8±4.9
Systolic blood pressure (mmHg) (mmHg)	116.6 ± 8.3	118.4±16.5	119.6±20.1	117.6±13.9
Diastolic blood pressure (mmHg)	80.3 ± 4.8	77.9±10.2	81.5±12.3	75.1±7.7
Aortic strain	0.127± 0.070	0.059±0.049*	0.079±0.061	0.042±0.027*†
Aortic distensibility (cm2/dynes 10–6)	4.89 ± 2.82	2.51±2.51*	3.48±3.29	1.74±1.38
Aortic stiffness index	5.89 ± 5.58	12.8±11.3*	7.68±4.62	16.9±13.4*†

*** p<0.05 vs. controls, † p<0.05 vs. etrTOF**

Abbreviations: cTOF: corrected tetralogy of Fallot, etrTOF: early total reconstruction for patients with TOF, pcTOF: early pallication, late correction for patients with TOF, LA: left atrial, LV: left ventricular

3DSTE-derived LV rotational mechanics. Sixteen out of 26 cTOF patients showed normally directed LV rotational mechanics, while apical and basal LV rotations were in the same clockwise or counterclockwise directions in 7 and 3 cTOF cases, respectively (10 out of 26, 38%) (Table 9). This sort of LV movement is called as LV rigid body rotation (RBR). The ratio of LV-RBR between etrTOF and pcTOF patients did not differ significantly (33% vs. 43%, p=0.70). cTOF patients with LV-RBR were managed separately during assessments.

Normally directed LV rotational mechanics. Significantly reduced LV apical rotation and twist could be demonstrated in all cTOF patients with preserved LV basal rotation regardless of previous procedure (Table 9). pcTOF patients showed significantly reduced LV apical rotation as compared to that of etrTOF cases.

LV 'rigid body rotation'. From the 7 cTOF patients with clockwise LV-RBR, apical and basal LV rotation proved to be −6.8±5.0 and −4.8±2.3 degrees, respectively with LV apico-basal gradient of 4.3±3.3 degrees. Apical and basal LV rotations of particular etrTOF patients were −12.3 and −8.5 degrees, −5.1 and −2.0 degrees, respectively, while the same values of pcTOF patients proved to be −8.5 and −5.5 degrees, −1.6 and −6.9 degrees, −3.9 and −5.4 degrees, −0.9 and −2.2 degrees, −15.2 and −3.4 degrees, retrospectively. The mean LV apical and basal LV rotation of 3 cTOF patients with counterclockwise LV-RBR proved to be 2.6±2.3 and 0.7±0.3 degrees, respectively with apico-basal gradient of 1.9±2.4 degrees. Apical and basal LV rotations of etrTOF patients were 5.9 and 0.7 degrees, 1.2 and 1.1 degrees, respectively, while the same values of the pcTOF patients proved to be 0.7 and 0.4 degrees. In this cohort of patients with LV-RBR, LV apico-basal gradient had no relationship with QRS duration, LA size, LV diastolic parameters, hypertension, arrhythmia, exercise capacity, TR and PR.

Table 10 Comparison of three-dimensional speckle-tracking echocardiography-derived left ventricular rotational mechanics in patients with tetralogy of Fallot and in controls

	Controls (n= 37)	All cTOF (n=26)	etrTOF (n= 12)	pcTOF (n=14)
Normally directed LV rotational mechanics (%)	37 (100)	16 (62)	8 (66)	8 (57)
Clockwise LV-RBR (%)	0 (0)	7 (27)	2 (16)	5 (35)
Counterclockwise LV-RBR (%)	0 (0)	3 (11)	2 (16)	1 (7)
Normally directed LV rotational mechanics				
LV basal rotation (degree)	-4.4±2.8	-3.9±2.3	-3.4±2.2	-4.3±2.4
LV apex rotation (degree)	10.2±4.5	5.2±3.7*	7.1±2.5*	3.2±3.7*†
LV twist (degree)	14.6±4.9	9.0±3.3*	10.5±2.8*	7.6±3.2*
LV twist time (ms)	337±94	361±108	321±69.5	402±128

*** p<0.05 vs. controls, † p<0.05 vs. etrTOF**

Abbreviations: cTOF: corrected tetralogy of Fallot, etrTOF: early total reconstruction for patients with TOF, pcTOF: early pallication, late correction for patients with TOF, LV: left ventricular, 3DSTE: three-dimensional speckle-tracking echocardiography, RBR: rigid body rotation

Correlations. Significant correlations could be demonstrated between LV apical rotation and aortic stiffness index ($r=-0.55$, $p=0.03$) and aortic distensibility ($r=0.52$, $p=0.04$) in all cTOF patients with normally directed LV rotational mechanics. No further correlations could be demonstrated between any other aortic elastic properties and LV rotational parameters in all cTOF groups and during subgroup analyses. No correlations were seen according to right bundle branch block or QRS-duration in ECG.

4.3. Tricuspid annular abnormalities following different surgical strategies in adults with corrected tetralogy of Fallot

Patient population. The present study comprised 24 adult patients with cTOF [mean age 32.8±13.5 years, 15 males (62%)]. Data of these patients' origin from a special registry for CHD patients (CSONGRAD Registry). Their results were compared with those of 33 age- and gender-matched healthy volunteers, who had no known disorders, diseases or other pathological conditions, risk factors, did not receive any drugs and showed negative echocardiographic and electrocardiographic findings. From the 24 adult cTOF patients, 12 had palliative surgery first [modified Blalock-Taussig (n=9), Waterston-Cooley (n=1) shunts, or Brock procedure (n=2)] (mean age at the palliation: 2.4±2.1 years, median age: 1.4 years, interquartile range: 3.5 years) followed by a late total correction (mean age at the total correction: 6.9±6.7 years, median age: 5.5 years, interquartile range: 6.5 years) (pcTOF group). Early total correction was performed in another 12 TOF patients (mean age at the repair: 3.9±3.1 years, median age: 5.0 years, interquartile range: 5.0 years) (etrTOF group). Demographic data and risk factors and their distribution in the cTOF group and subgroups and in controls are presented in Table 10.

Two-dimensional echocardiographic data. Left atrial and LV dimensions in controls and in patients with cTOF and in subgroups are presented in Table 1. TAPSE proved to be 18.7±3.2 mm in cTOF patients, which did not differ between etrTOF and pcTOF patients (18.8±2.0 vs. 18.6±4.1 mm, p=ns). Valvular regurgitations and their severity expressed in grades are presented in Table 1. Mean RV pressure was 14.3±2.1 mmHg without residual pulmonary stenosis or narrowing of a pulmonary artery branch.

Table 11 Baseline demographic and two-dimensional Doppler echocardiographic data in patients with tetralogy of Fallot and controls

	Controls (n= 33)	All cTOF (n= 24)	etrTOF (n= 12)	pcTOF (n= 12)
Risk factors				
Age (years)	36.7 ± 7.2	32.8 ± 13.5	32.6 ± 14.5	33.7 ± 15.0
Male gender (%)	15 (45)	9 (41)	7 (58)	3 (25)
Hypertension (%)	0 (0)	5 (22)	2 (17)*	4 (33)*
Diabetes mellitus (%)	0 (0)	0 (0)	0 (0)	0 (0)
Hypercholesterolaemia (%)	0 (0)	1 (4)	0 (0)	1 (8)
Two-dimensional echocardiography				
LA diameter (mm)	38.4 ± 3.2	41.3 ± 6.5	41.2 ± 7.2	41.3 ± 6.0
LV end-diastolic diameter (mm)	48.5 ± 2.8	50.1 ± 14.1	47.3 ± 5.6	47.9 ± 5.6
LV end-diastolic volume (ml)	108.7 ± 19.4	106.8 ± 30.3	107.8 ± 29.9	107.8 ± 29.9
LV end-systolic diameter (mm)	32.1 ± 2.1	30.7 ± 5.7	30.7 ± 5.1	30.7 ± 6.4
LV end-systolic volume (ml)	37.9 ±7.0	38.0 ± 19.9	37.7 ± 20.0	38.4 ± 20.6
Interventricular septum (mm)	9.2 ± 1.0	9.8 ± 1.5	9.5 ± 1.1	10.1 ± 1.9
LV posterior wall (mm)	8.9 ± 1.0	9.5 ± 1.4	9.3 ± 1.4	9.8 ± 1.4
LV ejection fraction (%)	65.1 ±2.4	65.5 ± 8.7	65.5 ± 6.3	65.5 ± 10.9
Mitral regurgitation				
grade 1 (%)	0 (0)	13 (54)*	5 (41)*	8 (75)*
grade 2 (%)	0 (0)	2 (8)	1 (8)	1 (8)
Tricuspid regurgitation				
grade 1 (%)	0 (0)	9 (37)*	6 (50)*	3 (25)*
grade 2 (%)	0 (0)	11 (46)*	5 (42)*	6 (50)*
grade 3 (%)	0 (0)	1 (4)	1 (8)	0 (0)
grade 4 (%)	0 (0)	2 (8)	0 (0)	2 (16)*

*** p<0.05 compared to controls, † p<0.05 compared to etrTOF patients**

Abbreviations: LA: left atrial, LV: left ventricular, TOF: tetralogy of Fallot, etrTOF: TOF – early total reconstruction, pcTOF: TOF – early palliation, late correction

Three-dimensional speckle-tracking echocardiography. Dilated end-systolic and end-diastolic TA morphologic parameters and their BSA-indexed counterpart could be detected in cTOF patients as compared to controls (Table 11). TAFAC and TAFS proved to be reduced in cTOF patients as well as in etrTOF and pcTOF patients compared to controls. None of TA morphologic and functional parameter showed any differences between etrTOF and pcTOF patients. Increased maximum (64.0±32.1 vs. 36.9±9.5 mL, P<0.05), preatrial contraction (56.2±30.9 vs. 30.5±9.3 mL, P<0.05) and minimum (48.6±31.9 vs. 24.0±8.4 mL, P<0.05) RA volumes could be detected in cTOF patients

Correlations. End-diastolic TAD and TAA correlated with Vmax (r=0.58, p=0.05 and r=0.63, p=0.04, respectively), VpreA (r=0.50, p=0.05 and r=0.57, p=0.04, respectively) and Vmin (r=0.76, p=0.03 and r=0.76, p=0.05, respectively). Similarly, end-systolic TAD and TAA correlated with Vmax (r=0.57, p=0.05 and r=0.63, p=0.05, respectively), VpreA (r=0.59, p=0.03 and r=0.55, P=0.05, respectively) and Vmin (r=0.76, p=0.04 and r=0.73, p=0.05, respectively), as well. End-diastolic and end- systolic TAP showed correlations with Vmin only (r=0.56, p=0.05 and r=0.66, p=0.04, respectively). Only TAFS correlated with Vmin (r=−0.45, p=0.05), other correlations between TA functional properties and RA volumes could not be detected. No correlations could be demonstrated between TAPSE and 3DSTE-derived TA dimensions and functional properties (TAFAC, TAFS) in cTOF patients.

Table 12 Comparison of three-dimensional speckle-tracking echocardiography-derived tricuspid annular morphological and functional parameters between adult patients with tetralogy of Fallot and controls

Data	Controls (n= 33)	All cTOF (n= 24)	etrTOF (n= 12)	pcTOF (n= 12)
Morphological parameters				
TAD-D (cm)	2.15 ± 0.23	2.74 ± 0.45*	2.77 ± 0.52*	2.71 ± 0.38*
TAD-D/BSA (cm/m^2)	1.18 ± 0.16	1.54 ± 0.31*	1.47 ± 0.24*	1.61 ± 0.37*
TAA-D (cm^2)	6.91 ± 1.20	9.82 ± 3.14*	9.86 ± 3.76*	9.78 ± 2.53*
TAA-D/BSA (cm/m^2)	3.78 ± 0.74	5.51 ± 1.70*	5.21 ± 1.63*	5.81 ± 1.79*
TAP-D (cm)	10.17 ± 1.51	12.26 ± 1.72*	12.15 ± 2.11*	12.38 ± 1.31*
TAP-D/BSA (cm/m^2)	5.58 ± 1.01	6.90 ± 1.30*	6.48 ± 1.00*	7.33 ± 1.45*
TAD-S (cm)	1.78 ± 0.16	2.45 ± 0.48*	2.48 ± 0.56*	2.41 ± 0.39*
TAD-S/BSA (cm/m^2)	0.98 ± 0.11	1.38 ± 0.31*	1.32 ± 0.26*	1.43 ± 0.35*
TAA-S (cm^2)	5.25 ± 1.21	7.98 ± 2.62*	8.16 ± 3.20*	7.80 ± 2.02*
TAA-S/BSA (cm/m^2)	2.87 ± 0.69	4.48 ± 1.43*	4.30 ± 1.37*	4.66 ± 1.53*
TAP-S (cm)	8.93 ± 0.97	10.88 ± 1.55*	10.78 ± 1.90*	10.98 ± 1.20*
TAP-S/BSA (cm/m^2)	4.91 ± 0.78	6.12 ± 1.19*	5.75 ± 0.92*	6.50 ± 1.34*
Functional parameters				
TAFAC (%)	24.08 ± 16.72	18.72 ± 6.99*	17.52 ± 6.85*	19.93 ± 7.21
TAFS (%)	16.72 ± 6.46	10.93 ± 5.68*	10.65 ± 6.09*	11.21 ± 5.50*

***p < 0.05 vs. Controls †< 0.05 vs. etrTOF**

Abbreviations: TAA-D: end-diastolic tricuspid annular area, TAA-S: end-systolic tricuspid annular area, TAD-D end-diastolic tricuspid annular diameter, TAD-S: end-systolic tricuspid annular diameter, TAFAC: tricuspid annular fractional area change, TAFS: tricuspid annular fractional shortening, TAP-D:end-diastolic tricuspid annular perimeter, TAP-S: end-systolic tricuspid annular perimeter, TOF: tetralogy of Fallot, etrTOF: TOF – early total reconstruction, pcTOF: TOF – early palliation, late correction

4.4. Multimodality imaging of adult patients with surgically corrected tetralogy of Fallot.

Patient population. The study comprised 17 patients with TOF (mean age: 28.6 ± 10.4 years; 10 males), recruited from the CSONGRAD Registry. Of the 17 patients with TOF included in the study, 10 underwent early complete reconstruction, while 7 underwent early palliation (all with modified Blalock-Taussig shunt surgery) followed by complete correction (Table 13). Patients who underwent early complete reconstruction had surgery at 5.1 ± 4.5 years of age, while patients in the other subgroup were 3.2 ± 3.4 years of age at the time of palliation, followed by complete correction at 10.0 ± 8.3 years of age. In the case of early complete reconstruction, 5 patients had a post RV outflow tract patch-repair status, while another 5 patients had a post homograft implantation status at the time of the study. For patients who underwent early palliation followed by late correction, the same numbers were 3 and 4. There were no significant differences between the two subgroups in the functional stage of heart failure according to the New York Heart Association or in the distance walked during the 6-minute walk test. No residual VSD was detected in either patient group. No significant co-morbidities were known in the cTOF population, with 1 patient having well-controlled hypertension. In terms of cardiovascular drug therapy, 1 patient was on anticoagulation with acenocoumarol, 2 patients were on mineralocorticoid antagonist therapy, 2 patients were on angiotensin-converting enzyme inhibitor therapy, and 3 patients were on ß-blocker therapy.

Table 13. Clinical data of the Tetralogy of Fallot patient population studied

	All cTOF	**etrTOF**	**pcTOF**	**p**
Patient number	17	10	7	**ns**
Male (%)	10 (59)	8 (80)	2 (29)	ns
Age at time of examination (years)	28.59 ± 4.63	25.01 ± 8.04	33.71 ±11.79	ns
Age at first surgery (years)	4.46 ±4.14	5.10 ± 4.51	3.20 ± 3.35	ns
Age at time of full correction (years)	6.94 ± 6.39	5.10 ± 4.51	10.00 ± 8.25	**0.014**
NYHA class	1.28 ± 0.57	1.30 ± 0.67	1.25 ± 0.5	**ns**
6MWT (m)	463.3 ± 71.6	443.7 ± 55.6	483.3 ± 106.9	**ns**

Abbreviations: TOF: tetralogy of Fallot; 6MWT: 6-minute walk test; ns: not significant; NYHA stage: New York Heart Association functional stage classification of heart failure

Echocardiographic and cMR data of the left heart. The LA showed no differences between the two subgroups. While routine LV dimensions measured during echocardiography did not differ between the two subgroups, LV end-systolic and end-diastolic volume index, LV end-diastolic volume, LV stroke volume and stroke volume index measured by cMR were lower in patients undergoing early total re-construction. LV-EF regardless of imaging modality, was found to be higher in cTOF patients who underwent early complete reconstruction, with the difference reaching significance level for echocardiographic measurements. Other parameters, including LV muscle mass, did not differ between subgroups (Table 13). There was no significant MR, reaching moderate in any of the patients. Mild MR was seen in 5 patients (50%) after complete reconstruction and in 4 patients (57%) after early palliation/late correction. No abnormal pressure gradient or significant regurgitation above the aortic valve was seen. Mild regurgitation was demonstrated in 2 (20%) and 6 (85%) cases in the two TOF subgroups. Table 14

Echocardiographic and cMR data of the right heart. RV echocardiographic dimensions did not differ between the two subgroups. Similarly, the RV dimensions measured during cMR did not differ in patients undergoing early complete reconstruction and early palliation/late complete correction. However, RV muscle mass and muscle mass index were higher in patients undergoing early complete reconstruction (Table 14). In both subgroups, TR was not significantly different in frequency. In etrTOF, 2 patients (20%) had moderate TR, 5 patients (50%) mild, while in pcTOF 2 patients (28%) had moderate TR and 4 patients (57%) mild. The degree of pulmonary stenosis did not differ between the two subgroups, and peak flow velocity measured by cMR (2.48 ± 0.95 m/s vs. 2.52 ± 1.37 m/s, (p = ns) and peak gradient measured by echocardiography (35.5 ± 18.0 mm Hg vs. 33.6 ± 13.8 mm Hg, p = ns) were not significantly different. The PR rate based on the regurgitant fraction measured by cMR did not differ significantly between the two groups (25.8 ± 17.8% vs. 26.5 ± 17.2%, p = ns). Table 15

Table 14. Left heart echocardiography and cardiac magnetic resonance imaging findings in corrected tetralogy of Fallot

	All cTOF (n=17)	etrTOF (n=10)	pcTOF (n=7)	p
Cardiac magnetic resonance imaging				
	52.47 ± 7.4	53.6 ± 8.21	50.86 ± 6.31	ns
LV EF (%)	60.2 ± 10	63.33 ± 9.09	55.5 ± 10.63	ns
	84.24 ± 27.19	76.3 ± 20.8	95.57 ± 32.69	ns
LV ESV (ml)	56.6 ± 27.32	47.17 ± 16.75	70.75 ± 36.43	ns
LV ESV Index (ml/m^2)	47.76 ± 16.71	40.5 ± 10.55	58.14 ± 19.07	**0.013**
	34 ± 17.59	26 ± 9.27	46 ± 21. 57	**0.037**
	174.82 ± 36.24	162.3 ± 20.88	192.71 ± 47.05	**0.044**
LV EDV (ml)	137.5 ± 34.28	126.5 ± 12.91	154 ± 51.4	ns
LV EDV Index (ml/m^2)	99 ± 23.11	86.6 ± 12.62	116.70 ± 23.7	**0.002**
	81.3 ± 23.7	69.33 ± 11.48	99.25 ± 27.37	**0.021**
	90.65 ± 14.79	86.1 ± 9.33	97.14 ± 19.2	**0.067**
LV SV (ml)	81.1 ± 12.56	79.33 ± 4.68	83.75 ± 20.53	ns
	51.12 ± 9.19	46 ± 6.77	58.43 ± 7.11	**0.001**
LV SV Index (ml/m^2)	48.6 ± 10.36	43.5 ± 7.23	56.25 ±10.24	**0.024**
	103.69 ± 28.81	103.11 ± 23.68	104.43 ± 36.42	ns
LV mass (g)	136.5 ± 38.6	137.17 ± 31.59	135.5 ± 52.96	ns
	57.69 ± 12.78	54.11 ± 8.57	62.29 ± 16.33	ns
LV mass index (g/m^2)	78.6 ± 18.03	73.83 ± 13.35	85.75 ± 23.77	ns
Two-dimensional echocardiography				
LA diameter 1 (mm)	33.5 ± 4.97	34.88 ± 4.16	31.67 ± 5.75	ns
LA diameter 2 (mm)	40.71 ± 7.5	41.5 ± 9.21	39.67 ± 5.01	ns
LA diameter 3 (mm)	38.11 ± 2.62	36.75 ± 2.36	39.2 ± 2.49	ns
LV EDV (ml)	117 ± 22.8	113 ± 17.86	122.33 ± 29.08	ns
LV ESV (ml)	41.57 ± 19.63	35.13 ± 12.68	50.17 ± 24.93	ns
LV EF (ml)	66.29 ± 8.48	69.75 ± 6.8	61.67 ± 8.8	**0.038**
IVS (mm)	9.86 ± 1.79	9.5 ± 1.69	10.33 ± 1.97	ns
PW (mm)	9.36 ± 1.69	9.38 ± 1.85	9.33 ± 1.63	ns

Abbreviations: LV: left ventricle; LA: left atrium; EDV: end-diastolic volume; EF: ejection fraction; ESV: end-systolic volume; IVS: interventricular septal thickness; ns: not significant; PW: LV posterior wall thickness; SV: stroke volume

Table 15. Results of right heart echocardiography and cardiac magnetic resonance imaging in corrected tetralogy of Fallot

	All cTOF (n=17)	etrTOF (n=10)	pcTOF (n=7)	p
Cardiac magnetic resonance imaging				
RV EF (%)	43.53 ± 9.69	42.70 ± 9.43	44.71 ± 10.69	ns
	51.50 ± 10.62	48.67 ± 9.54	55.75 ± 11.03	ns
RV ESV (ml)	157.59 ± 60.08	160.10 ± 56.20	154.0 ± 69.73	ns
	95.40 ± 34.17	104.67 ± 32.18	81.50 ± 36.70	ns
RV ESV Index (ml/m^2)	86.65 ± 28.71	83.90 ± 24.38	90.57 ± 35.73	ns
	54.20 ± 16.21	56.50 ± 15.25	50.75 ± 19.33	ns
RV EDV (ml)	273.58 ± 77.89	273.80 ± 62.29	273.29 ± 101.77	ns
	194.90 ± 59.51	203.83 ± 50.04	181.50 ± 77.79	ns
RV EDV Index (ml/m^2)	152.06 ± 37.43	145.20 ± 28.42	161.86 ± 48.31	ns
	111.60 ± 27.38	109.83 ± 22.21	114.25 ± 37.56	ns
RV SV (ml)	116.06 ± 35.05	113.90 ± 26.30	119.14 ± 47.11	ns
	99.50 ± 36.58	99.17 ± 32.48	100.00 ± 47.49	ns
RV SV Index (ml/m^2)	65.29 ± 19.35	61.00 ± 14.88	71.43 ± 24.33	ns
	57.40 ± 18.76	53.33 ± 14.79	63.50 ± 24.66	ns
RV muscle mass (g)	63.93 ± 23.33	72.33 ± 21.03	51.33 ± 22.33	**0.044**
	122.70 ± 45.83	145.00 ± 35.12	89.25 ± 41.93	**0.026**
RV muscle mass index (g/m^2)	32.80 ± 7.83	33.89 ± 5.33	31.17 ± 11.00	ns
	69.50 ± 21.53	78.50 ± 18.10	56.00 ± 20.99	**0.054**
Two-dimensional echocardiography				
RA diameter 1 (mm)	47.62 ± 7.15	48.75 ± 6.98	45.80 ± 7.82	ns
RA diameter 2 (mm)	47.83 ± 8.39	45.86 ± 6.09	50.60 ± 11.01	ns
RA area (mm^2)	18.17 ± 6.06	17.58 ± 4.81	18.86 ± 7.70	ns
RV basal diameter (mm)	52.21 ± 6.86	52.63 ± 6.30	51.67 ± 8.14	ns
RV diameter at the papillary muscles (mm)	42.14 ± 7.12	44.63 ± 6.44	38.83 ± 7.14	ns
RV length (mm)	79.36 ± 10.53	81.63 ± 13.37	76.30 ± 4.32	ns
RV pressure (mmHg)	39.17 ± 15.82	38.50 ± 0.71	39.50 ± 20.40	ns
TAPSE (mm)	17.00 ± 3.49	16.33 ± 3.56	17.67 ± 3.61	ns
Inferior Vena Cave during expiration (mm)	14.89 ± 3.41	15.83 ± 2.79	13.00 ± 4.36	ns

Abbreviations: EDV: end-diastolic volume; EF: ejection fraction; ESV: end-systolic volume; RV: right ventricle; RA: right atrium; ns : not significant; SV: stroke volume; TAPSE: tricuspid annular plane systolic excursion

5. Discussion

5.1. Left ventricular strains correlate with aortic elastic properties in adult patients with corrected tetralogy of Fallot

To the best of the authors' knowledge, the relationship between 3DSTE-derived LV strains and aortic elastic properties has not been simultaneously examined, and their correlation has never been investigated in cTOF patients. Theoretically cardiovascular risk factors could have effects on LV deformation and aortic size and function at the same time. However, there are interactions between the LV and the arterial system as well, called ventricular-arterial coupling, the LV and the arterial system have effects on each other. In recent studies, aortic elasticity properties showed correlations with LV-CS and LV rotational parameters even in healthy subjects [14, 17].

It has already been demonstrated that cTOF—even with preserved LV-EF—exhibits reduced global LV-LS and LV-CS measured by 2DSTE. This suggests that there is an underlying subclinical LV damage even after surgical repair [6]. Furthermore, it has also been found that abnormal global LV-LS and RV-LS and LV rotation are associated with adverse cardiovascular events, highlighting the potential clinical usefulness of STE-derived parameters determining prognosis, and finding, which patients are at high risk [18]. Aortic dilation is also a known abnormality in cTOF, which is associated with higher ASI [4]. This was confirmed by both M-mode echocardiography- and novel 2DSTE-derived aortic stiffness parameters [19]. Our results confirm previous studies describing that cTOF is associated with impaired LV deformations [20, 21]. Importantly, not only the widely used 2DSTE-derived LV-LS proved to be the most robust. LV-AS, and most notably LV-CS are significantly impaired in cTOF patients, highlighting the clinical significance of 3DSTE having the capability of simultaneous assessment of all LV strain values at the same time from the same 3D dataset in complex CHDs. Interestingly, patients who underwent early total correction for TOF have mostly preserved global, mean segmental, and regional strains, with mean segmental LV-RS and LV-3DS being supernormal in certain cases.

These supernormal values might be part of a preclinical compensatory mechanism before manifest deterioration of LV function, but to confirm these suspicions, longitudinal studies are warranted. Another important finding is that for cTOF patients with pcTOF, all global and mean segmental strain values were mostly significantly reduced compared to both controls and etrTOF subjects. For segmental strains, these differences were similarly present. A notable finding in segmental strain analysis is that mostly septal segments had significantly lower LV strains in pcTOF patients. This finding is most likely explained by the nature of TOF, the longer presence of the VSD,

and the interventricular septal patch. Correlations could also be presented in cTOF patients between LV strains and aortic stiffness parameters, and those correlations were present during subgroup analysis, as well. These results confirm strong effects of ventricular-arterial coupling in these patients in spite of the above presented abnormalities.

Limitations. There are some limitations, which can be considered important to be taken into account when interpreting results:

- Currently 3DSTE has lower temporal and spatial resolution than 2D echocardiography, therefore image quality is worse.
- It was not aimed to validate 3DSTE parameters due to their validated nature. Moreover, detailed analysis of other heart chambers was also not purposed to be performed.
- Interventricular and atrio-ventricular interactions are of high importance, the current study did not aim to evaluate them.
- A relatively small number of patients was investigated in a single adult CHD center. For better statistical strength, more patients could have been evaluated.

5.2. Left ventricular rotational abnormalities in adult patients with corrected tetralogy of Fallot following different surgical procedures

In spite of rapid development in cardiovascular imaging, echocardiography is still the basic imaging modality due to its non-invasiveness, relatively good image quality, reproducibility and short learning-curve [13, 22]. Moreover, it allows simultaneous assessment of cardiovascular abnormalities like aortic elastic properties by M-mode echocardiography and LV rotational mechanics by 3DSTE [22, 23]. Aortic stiffness describes elasticity of the aorta which sets against its distension [23]. In normal situations, basal and apical LV regions rotate in opposite directions: while LV apex rotates in counterclockwise direction, LV base rotates in clockwise direction resulting in a ‘towel-wringing motion’-like movement called LV twist [24]. It is known that aortic stiffness correlates with LV rotational parameters in healthy subjects, larger aortic stiffness is associated with increased LV apical rotation and twist suggesting an early compensating mechanism [14]. Moreover, both increased aortic stiffness [19] and LV rotational abnormalities [20, 25] could be detected in cTOF. However, their relationship and the effect of different treatment strategies on these parameters have never been investigated.

According to the present findings, it could be stated that high ratio of cTOF patients showed LV-RBR (38%). In a recent study by Menting et al., 11 and 2 out of 82 (13% and 2%, respectively) cTOF patients had reversed or absent LV apical rotation (clockwise LV-RBR), while 9 and 6 out of

82 (11% and 7%, respectively) showed reversed or absent LV basal rotation (counterclockwise LV-RBR) [20]. The same parameters proved to be 27% and 11% in the present study with a smaller population. In the study of Dragulescu et al., 19 of 50 young cTOF patients had reversed (counterclockwise) LV basal rotation [25]. According to the literature, LV-RBR was found to be a frequent phenomenon in several disorders with the largest ratio in non-compaction (50–100%) [26], dilated (50%) [27] and hypertensive cardiomyopathies (32%) [28], cardiac amyloidosis (60%) [29] and acromegaly (20%) [30]. Some case reports showed LV-RBR in some CHDs as well including Ebstein's anomaly [31], univentricular heart [32] and hypoplastic right-heart syndrome [33]. Eight out of 82 (10%) cTOF patients had reduced LV apical rotation in the study by Menting et al. [20]. In our study, the majority of cTOF patients had no LV-RBR (62%). Although direction of LV rotational mechanics proved to be normal in these patients, LV apical rotation was significantly reduced as compared to that of controls. Moreover, the impairment proved to be more pronounced in pcTOF patients. LV apical rotation was reduced, but not reversed in the study of Dragulescu *et al.* [25]. In our study, LV basal rotation proved to be preserved. According to the results of van Grootel et al., reduced LV apical rotation is associated with worse outcomes in cTOF patients [18]. In the present study, significantly impaired aortic elastic properties could be demonstrated in cTOF patients in agreement with previous findings [19].

When correlations were examined with LV rotational abnormalities, aortic elastic properties negatively correlated with LV apical rotation suggesting that increased aortic stiffness is associated with reduced LV apical rotation. These results are the opposite of those found in healthy subjects, where increased aortic stiffness showed positive correlations with LV apical rotation: the higher the aortic stiffness was, the higher the LV apical rotation was [14, 17]. These results suggest that although normally directed LV rotational mechanics could be seen in most cases, not only reduced LV apical rotation could be detected, but the compensating effect of LV rotational mechanics as seen in healthy subjects was absent in cTOF patients without LV-RBR. Although changes in RV dimensions are associated with abnormal LV flows and volumes suggesting significant interventricular interactions, the present study did not aim to examine in detail [34].

The above-mentioned results suggest several facts. In agreement with the recent findings, LV rotational mechanics can be non-invasively assessed by 3DSTE [22], for which normal reference values are also available [35]. Although the results are contradictory with previous findings [20, 25], significant LV rotational abnormalities could be detected in cTOF including LV-RBR and impairment of apical LV rotation. When different treatment strategies were compared, beneficial results could be found in patients with etrTOF corresponding with recent findings [36]. Finally, abnormal physiologic response of LV rotational mechanics to increased aortic stiffness could be

detected in cTOF patients without LV-RBR suggesting that the LV rotational mechanics have no ability to compensate for aortic stiffness. However, due to the facts that relatively low number of cTOF patients were examined and results are conflicting with current findings, further studies are warranted to confirm present results.

Limitations. Over the previously mentioned limitations, the followings should be considered:

- LV rotational abnormalities were examined in adult cTOF patients. However, children with cTOF could show different results.
- 3DSTE has inferior temporal and spatial resolution when compared to 2D echocardiography, which could affect the results.
- The present study focused on the relationship between LV rotational abnormalities and aortic stiffness. Interventricular interaction was not evaluated by the current study.
- Echocardiographic measurement of aortic dimensions involves some inaccuracies, which could be taken into consideration when interpreting results.

5.3. Tricuspid annular abnormalities following different surgical strategies in adults with corrected tetralogy of Fallot

To the best of the authors' knowledge, this is the first time to examine 3DSTE-derived tricuspid annulus (TA) abnormalities in adult cTOF patients and their relationship with right atrial (RA) volumes. Several disorders like cTOF itself may lead to functional tricuspid regurgitation (FTR) through TA dilation. Minimum RA volume and TA area were directly correlated to FTR severity [37]. Moreover, RA volume was found to be a major determinant of TA area, and RA enlargement is an important mechanism of TA dilation in FTR irrespective of the cardiac rhythm and RV loading conditions [38]. In a recent 3DSTE study, detailed analysis showed increased RA volumes with reduced RA emptying fractions together with unchanged RA stroke volumes respecting the cardiac cycle in cTOF patients [39].

In the present study, FTR was significantly common in cTOF patients with more pronounced presence in pcTOF cases. Both end- diastolic and end-systolic TA dimensions were found to be dilated in cTOF as compared to those of controls and were accompanied with TA functional impairment. No differences could be demonstrated, however, in TA morphological and functional properties according to the surgical procedure performed. Moreover, strong correlations could be demonstrated between RA volumes and TA dimensions in cTOF suggesting a determinative relationship between these parameters. Old-fashioned M-mode echocardiography and the most recent

3DSTE together allows complex spatial analysis of the TA movement thought the cardiac cycle. Vertical movement of the TA represented by TAPSE and decreased horizontal 'sphincter-like' TA motion represented by TAFAC and TAFS did not correlate with each other in cTOF in this study. These results could suggest complexity of deterioration of TA functions in cTOF, which requires further examinations on the right heart function. According to the surgical procedures used for TOF corrections, beneficial results could be demonstrated in recent studies related to LV contractility represented by LV strains [40] and LV rotational mechanics [41] and mitral annulus (MA) morphology and function [36] in etrTOF patients compared to pcTOF patients. Similar findings could not be detected in TA parameters between the subgroups examined. These results could suggest fixed clinical situation on the right heart, but further studies are warranted to confirm our findings.

Limitations. The following limitations not mentioned so far should be taken into account:

- 2D echocardiography has higher temporal and spatial resolution than 3DSTE, which could affect the results.
- The normal reference values of 3DSTE-derived TA parameters were not available in the literature at time of the publication of the study.

5.4. Multimodality imaging of adult patients with surgically corrected tetralogy of Fallot.

Modern non-invasive cardiovascular imaging techniques allow relatively simple examination of the heart and the large vessels, even in pathologies with complex structural abnormalities such as CHD. However, routine two-dimensional Doppler echocardiographic studies have limited capabilities in the analysis of certain cardiac structures, where cMR can provide substantial help by enabling detailed and accurate analysis due to its good image quality [1, 42]. TOF is one of the most common CHD [1, 43]. Without surgery, life expectancy is limited, and cyanosis occurs rapidly without surgery due to right-to-left shunting due to pulmonary stenosis. Two main surgical strategies have been used in the management of TOF. One is early palliation followed by a delayed correction, the other is the early complete reconstruction [1, 2]. To understand the advantages and disadvantages of each surgical strategy on the physical condition and survival of patients, long-term comparative studies are needed.

Our results on the left side of the heart suggest that the LV is more dilated, function is reduced and blood volume is increased in pcTOF compared to etrTOF patients during late follow-up. The above differences may be due to LV volume overload caused by systemo-pulmonary shunting, the duration and magnitude of which is related to LV dilatation. Accordingly, previous studies have already suggested the benefits of early complete reconstruction in this patient group [44]. In the

presence of cTOF, although significant LV deformation abnormalities can be detected and LV contractility 'strain' is reduced and correlated with aortic stiffness, etrTOF patients have a more favourable LV 'strain' compared to pcTOF [40]. In addition to the above, significant LV rotational abnormalities have been demonstrated in the presence of cTOF, with abnormal physiological response correlated with aortic stiffness [41]. In addition, volumetric and 'strain' abnormalities affecting all left atrial functions can be detected [45]. Mitral annulus dilatation and functional impairment are independent of the type of correction, but pcTOF patients have worse outcomes [36]. In contrast to LV abnormalities, smaller RV abnormalities were demonstrated, which is important because RV size and function are of great importance in this patient population, both in relation to surgical indication and clinical status [1, 42].

Our results suggest that early complete reconstruction resulted in significantly greater RV muscle mass, which may be due to the timing of the first surgery performed later. In contrast to early palliation/late complete reconstruction, in early complete reconstruction, the RV is not initially unloaded by the shunt providing the small blood circuit circulation, and there is a continuous RV pressure load until the time of complete reconstruction, which may directly explain the development of hypertrophy [46]. However, according to a study published by O'Meagher et al. there is a positive correlation between RV muscle mass and the load-bearing capacity of individuals with cTOF [47]. It is known that the RA, the RV and the TA between them form an integral unit. Accordingly, the right atrium shows complex volumetric and functional differences in the presence of cTOF [39]. The TA is dilated, which is correlated with RA volumes, and its function TA size and function are similar in patients with TOF who have undergone either complete early reconstruction or early palliation/late complete correction [48]. The literature and our own results suggest a long-term benefit of earlier complete reconstruction in patients with TOF. TOF is a specific disease with a relatively small number of cases, so following the outcome of clinical practice, comparing surgical strategies used decades ago with modern protocols, allows future recommendations to be increasingly based on long-term outcomes and expert opinion.

Limitations. The following limitations not mentioned so far should be taken into account:

- The present study was a retrospective analysis of the results of cardiac imaging examinations conducted in routine clinical patient care, therefore the studies were not based on standardised protocols.
- Possible associations with residual pulmonary regurgitation or stenosis or other parameters were not investigated.

6. Conclusions (new observations)

Significant LV deformation abnormalities could be demonstrated in cTOF patients. etrTOF patients have beneficial LV strain parameters as compared to those of pcTOF patients. LV strains show correlations with echocardiography-derived aortic elastic properties in cTOF patients suggesting ventricular-arterial coupling.

Significant LV rotational abnormalities could be demonstrated in cTOF with high prevalence of LV-RBR. pcTOF patients showed significantly reduced LV apical rotation as compared to that of etrTOF cases. Unexpected abnormal physiologic response of LV rotational mechanics to increased aortic stiffness can be detected in cTOF patients without LV-RBR.

TA is dilated in cTOF with reduced function in adult patients with cTOF. TA dilation is related to RA volumes. etrTOF and pcTOF patients have similar TA dimensions and TA functional properties.

Beneficial LV morphological and functional parameters, but more pronounced RV hypertrophy could be detected in patients with cTOF following early total reconstruction as compared to that of subjects late after early palliation/late correction

7. References

1. Apitz, C., G.D. Webb, and A.N. Redington, Tetralogy of Fallot. Lancet, 2009. 374(9699): p. 1462-71.
2. Al Habib, H.F., et al., Contemporary patterns of management of tetralogy of Fallot: data from the Society of Thoracic Surgeons Database. Ann Thorac Surg, 2010. 90(3): p. 813-9; discussion 819-20.
3. Francois, K., Aortopathy associated with congenital heart disease: A current literature review. Ann Pediatr Cardiol, 2015. 8(1): p. 25-36.
4. Cruz, C., et al., Aortic dilatation after tetralogy of Fallot repair: A ghost from the past or a problem in the future? Rev Port Cardiol (Engl Ed), 2018. 37(7): p. 549-557.
5. Tan, J.L., et al., Intrinsic histological abnormalities of aortic root and ascending aorta in tetralogy of Fallot: evidence of causative mechanism for aortic dilatation and aortopathy. Circulation, 2005. 112(7): p. 961-8.
6. Mohammad Nijres, B., et al., Use of Speckle Tracking Echocardiography to Assess Left Ventricular Systolic Function in Patients with Surgically Repaired Tetralogy of Fallot: Global and Segmental Assessment. Pediatr Cardiol, 2018. 39(8): p. 1669-1675.
7. Li, Vivian Wing-Yi et al. Ventricular Myocardial Deformation Imaging of Patients with Repaired Tetralogy of Fallot. Journal of the American Society of Echocardiography: official publication of the American Society of Echocardiography. vol. 2020. 33(7): p. 788-801.
8. Zachos, Panagiotis et al. The value of myocardial strain imaging in the evaluation of patients with repaired Tetralogy of Fallot: a review of the literature. Heart Failure Reviews. 2023. 28(1): p. 97-112
9. Karnik, Ruchika et al. Abnormalities in Left Ventricular Rotation Are Inherent in Young Children with Repaired Tetralogy of Fallot and Are Independent of Right Ventricular Dilation. Pediatric Cardiology. 2018. 39(6). p. 1172-1180
10. Niwa, K., Aortopathy in Congenital Heart Disease in Adults: Aortic Dilatation with Decreased Aortic Elasticity that Impacts Negatively on Left Ventricular Function. Korean Circ J, 2013. 43(4): p. 215-20.
11. Yucel, E., et al., The tricuspid valve in review: anatomy, pathophysiology and echocardiographic assessment with focus on functional tricuspid regurgitation. J Thorac Dis, 2020. 12(5): p. 2945-2954.
12. Havasi, K., et al., [More than 50 years' experience in the treatment of patients with congenital heart disease at a Hungarian university hospital]. Orv Hetil, 2015. 156(20): p. 794-800.
13. Lang, R.M., et al., Recommendations for cardiac chamber quantification by echocardiography in adults: an update from the American Society of Echocardiography and the European Association of Cardiovascular Imaging. J Am Soc Echocardiogr, 2015. 28(1): p. 1-39 e14.
14. Nemes, A., et al., Correlations between echocardiographic aortic elastic properties and left ventricular rotation and twist--insights from the three-dimensional speckle-tracking echocardiographic MAGYAR-Healthy Study. Clin Physiol Funct Imaging, 2013. 33(5): p. 381-5.
15. Nemes, A. et al. Normal reference values of left ventricular strain parameters in healthy adults: Real-life experience from the single-center three-dimensional speckle-tracking echocardiographic MAGYAR-Healthy Study. Journal of Clinical Ultrasound : JCU, 2021. 49(4): p. 368-377
16. Kormányos, Á. et al. Normal values of left ventricular rotational parameters in healthy adults-Insights from the three-dimensional speckle tracking echocardiographic MAGYAR-Healthy Study. Echocardiography 2019. 36(4): p. 714-721

17. Zhang, J., et al., Relation of arterial stiffness to left ventricular structure and function in healthy women. Cardiovasc Ultrasound, 2018. 16(1): p. 21.
18. van Grootel, R.W.J., et al., The Prognostic Value of Myocardial Deformation in Adult Patients With Corrected Tetralogy of Fallot. J Am Soc Echocardiogr, 2019. 32(7): p. 866-875 e2.
19. Cruz, C., et al., Ascending aorta in tetralogy of Fallot: Beyond echocardiographic dimensions. Echocardiography, 2018. 35(9): p. 1362-1369.
20. Menting, M.E., et al., Abnormal left ventricular rotation and twist in adult patients with corrected tetralogy of Fallot. Eur Heart J Cardiovasc Imaging, 2014. 15(5): p. 566-74.
21. Li, S.N., et al., Left ventricular mechanics in repaired tetralogy of Fallot with and without pulmonary valve replacement: analysis by three-dimensional speckle tracking echocardiography. PLoS One, 2013. 8(11): p. e78826.
22. Nemes, A., et al., [Three-dimensional speckle-tracking echocardiography -- a further step in non-invasive three-dimensional cardiac imaging]. Orv Hetil, 2012. 153(40): p. 1570-7.
23. Nemes, A., et al., Echocardiographic evaluation and clinical implications of aortic stiffness and coronary flow reserve and their relation. Clin Cardiol, 2008. 31(7): p. 304-9.
24. Nakatani, S., Left ventricular rotation and twist: why should we learn? J Cardiovasc Ultrasound, 2011. 19(1): p. 1-6.
25. Dragulescu, A., et al., Effect of chronic right ventricular volume overload on ventricular interaction in patients after tetralogy of Fallot repair. J Am Soc Echocardiogr, 2014. 27(8): p. 896-902.
26. van Dalen, B.M., et al., Left ventricular solid body rotation in non-compaction cardiomyopathy: a potential new objective and quantitative functional diagnostic criterion? Eur J Heart Fail, 2008. 10(11): p. 1088-93.
27. Popescu, B.A., et al., Left ventricular remodelling and torsional dynamics in dilated cardiomyopathy: reversed apical rotation as a marker of disease severity. Eur J Heart Fail, 2009. 11(10): p. 945-51.
28. Maharaj, N., et al., Time to twist: marker of systolic dysfunction in Africans with hypertension. Eur Heart J Cardiovasc Imaging, 2013. 14(4): p. 358-65.
29. Nemes, A., et al., Different patterns of left ventricular rotational mechanics in cardiac amyloidosis-results from the three-dimensional speckle-tracking echocardiographic MAGYAR-Path Study. Quant Imaging Med Surg, 2015. 5(6): p. 853-7.
30. Kormanyos, A., et al., Left ventricular twist is impaired in acromegaly: Insights from the three-dimensional speckle tracking echocardiographic MAGYAR-Path Study. J Clin Ultrasound, 2018. 46(2): p. 122-128.
31. Nemes, A., et al., Left Ventricular Rigid Body Rotation in Ebstein's Anomaly from the MAGYAR-Path Study. Arq Bras Cardiol, 2016. 106(6): p. 544-5.
32. Nemes, A., et al., Can univentricular heart be associated with "rigid body rotation"? A case from the threedimensional speckle-tracking echocardiographic MAGYAR-path study. Hellenic J Cardiol, 2015. 56(2): p. 186-8.
33. Nemes, A., K. Havasi, and T. Forster, "Rigid body rotation" of the left ventricle in hypoplastic right-heart syndrome: a case from the three-dimensional speckle-tracking echocardiographic MAGYAR-Path Study. Cardiol Young, 2015. 25(4): p. 768-72.
34. Schafer, M., et al., Abnormal left ventricular flow organization following repair of tetralogy of Fallot. J Thorac Cardiovasc Surg, 2020. 160(4): p. 1008-1015.

35. Kormanyos, A., et al., Normal values of left ventricular rotational parameters in healthy adults-Insights from the three-dimensional speckle tracking echocardiographic MAGYAR-Healthy Study. Echocardiography, 2019. 36(4): p. 714-721.
36. Nemes, A., et al., Mitral annulus is enlarged and functionally impaired in adult patients with repaired tetralogy of Fallot as assessed by three-dimensional speckle-tracking echocardiography-results from the CSONGRAD Registry and MAGYAR-Path Study. Cardiovasc Diagn Ther, 2019. 9(Suppl 2): p. S221-S227.
37. Guta, A.C., et al., The Pathophysiological Link between Right Atrial Remodeling and Functional Tricuspid Regurgitation in Patients with Atrial Fibrillation: A Three-Dimensional Echocardiography Study. J Am Soc Echocardiogr, 2021. 34(6): p. 585-594 e1.
38. Muraru, D., et al., Right atrial volume is a major determinant of tricuspid annulus area in functional tricuspid regurgitation: a three-dimensional echocardiographic study. Eur Heart J Cardiovasc Imaging, 2021. 22(6): p. 660-669.
39. Nemes, A., et al., Evaluation of right atrial dysfunction in patients with corrected tetralogy of Fallot using 3D speckle-tracking echocardiography. Insights from the CSONGRAD Registry and MAGYAR-Path Study. Herz, 2015. 40(7): p. 980-8.
40. Racz, G., et al., Left ventricular strains correlate with aortic elastic properties in adult patients with corrected tetralogy of Fallot (Results from the CSONGRAD Registry and MAGYAR-Path Study). Cardiovasc Diagn Ther, 2021. 11(2): p. 611-622.
41. Nemes, A., et al., Left ventricular rotational abnormalities in adult patients with corrected tetralogy of Fallot following different surgical procedures (Results from the CSONGRAD Registry and MAGYAR-Path Study). Cardiovasc Diagn Ther, 2021. 11(2): p. 623-630.
42. Baumgartner, H., et al., 2020 ESC Guidelines for the management of adult congenital heart disease. Eur Heart J, 2021. 42(6): p. 563-645.
43. Bedair, R. and X. Iriart, EDUCATIONAL SERIES IN CONGENITAL HEART DISEASE: Tetralogy of Fallot: diagnosis to long-term follow-up. Echo Res Pract, 2019. 6(1): p. R9-R23.
44. Masutani, S., Left Ventricular End-Diastolic Dimension for the Assessment of the Pulmonary to Systemic Flow Ratio in Congenital Heart Diseases. Circ J, 2021. 86(1): p. 136-137.
45. Havasi, K., et al., Left Atrial Deformation Analysis in Patients with Corrected Tetralogy of Fallot by 3D Speckle-Tracking Echocardiography (from the MAGYAR-Path Study). Arq Bras Cardiol, 2017. 108(2): p. 129-134.
46. Ye, L., et al., Pressure Overload Greatly Promotes Neonatal Right Ventricular Cardiomyocyte Proliferation: A New Model for the Study of Heart Regeneration. J Am Heart Assoc, 2020. 9(11): p. e015574.
47. O'Meagher, S., et al., Right Ventricular Mass is Associated with Exercise Capacity in Adults with Repaired Tetralogy of Fallot. Pediatr Cardiol, 2015. 36(6): p. 1225-31.
48. Nemes, A., et al., Tricuspid annular abnormalities following different surgical strategies in adults with corrected tetralogy of Fallot (Results from the CSONGRAD Registry and MAGYAR-Path Study). Cardiovasc Diagn Ther, 2021. 11(6): p. 1276-1283.

8. Acknowledgements

The studies reported in this work were performed at the Department of Medicine, Cardiology Center, Division of Non-Invasive Cardiology (formerly 2nd Department of Medicine and Cardiology Center), Albert Szent-Györgyi Medical School, University of Szeged, Hungary.

First of all, I express my outmost gratitude to Prof. Dr. Attila Nemes for his continuous guidance during my work, who was my tutor and scientific adviser. Without his support and thesis would have not been performed.

I would like to thank very much also Prof. Dr. Tamás Forster, and Prof. Dr. Róbert Sepp and Dr. Tamás Szili-Török the former and current heads of the Cardiology Center, who supported me in my clinical and scientific work.

I am grateful to my current and former clinical mentors, Dr. Viktória Nagy and Dr. Kálmán Havasi who allowed me to flourish my passion for echocardiography.

I also owe my thanks to my fellow researchers. Dr. Árpád Kormányos, and Dr. Nándor Gyenes, working together and supporting each other's scientific work has been an important driving force.

I would like to also thank all co-authors.

I thank all my colleagues as well as nurses, assistants and all the members of the Institute for their day to day support.

Most importantly I am grateful for the continuous and steadfast support of my wife, without whom I'd never get anything done.

Photocopies of essential publications